ผลของการเติมทองแดงต่อสมบัติเทอร์โมอิเล็กทริกของบีตา-ไอรอนไดซิลิไซด์
ที่เตรียมด้วยการแอลลอยด์เชิงกล

นายภาณุวัฒน์ อรรถโชติศักดา

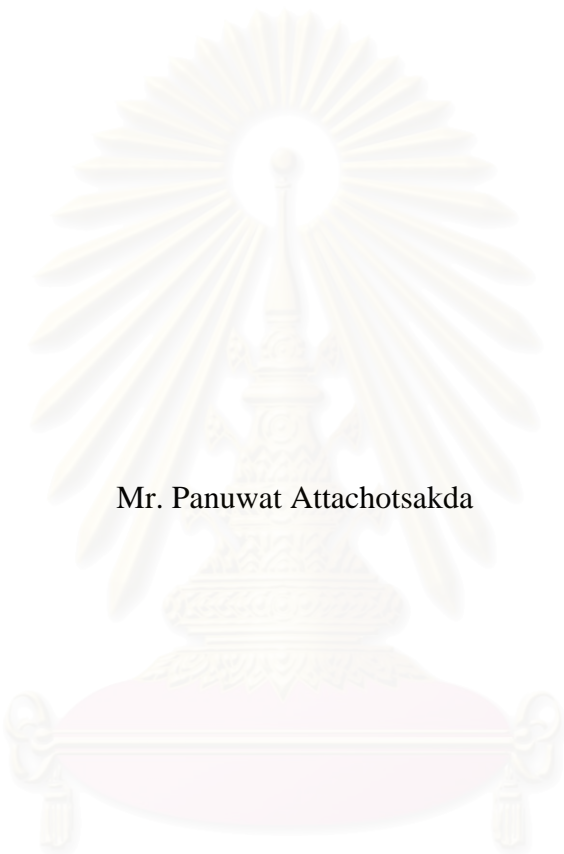EFFECTS OF COPPER ADDITION ON THERMOELECTRIC PROPERTIES OF

β-FeSi$_2$ PREPARED BY MECHANICAL ALLOYING

Mr. Panuwat Attachotsakda

A Thesis Submitted in Partial Fulfillment of the Requirements

for the Degree of Master of Science Program in Physics

Department of Physics

Faculty of Science

Chulalongkorn University

Academic Year 2006
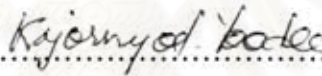
Thesis Title   EFFECTS OF COPPER ADDITION ON
           THERMOELECTRIC PROPERTIES OF β-FeSi$_2$
           PREPARED BY MECHANICAL ALLOYING

By   Mr. Panuwat Attachotsakda

Field of Study   Physics

Thesis Advisor   Somchai Kiatgamolchai, Ph.D.

Thesis Co-advisor   Siripan Nilpairach, Ph.D.

Accepted by the Faculty of Science, Chulalongkorn University in **Partial** Fulfillments of the Requirements for the Master's Degree

……………………………………………Dean of the Faculty of Science
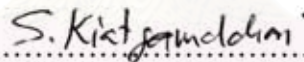
(Professor Piamsak Menasveta, Ph. D.)
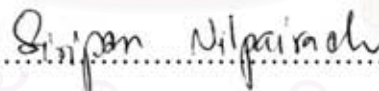
THESIS COMMITTEE

………………………………………….Chairman

(Assistant Professor Kajornyod Yoodee, Ph. D.)
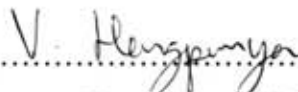
……………………………………………Thesis Advisor

(Somchai Kiatgamolchai, Ph. D.)

……………………………………………Thesis Co-advisor

(Siripan Nilpairach, Ph.D.)

…………………………………………....Member

(Tonphong Kaewkongka, Ph.D.)

………………………………………….Member

(Varagorn Hengpunya, Ph.D.)

ภาณุวัฒน์ อรรถโชติศักดา: ผลของการเติมทองแดงต่อสมบัติเทอร์โมอิเล็กทริกของบีตา-ไอรอนได ซิลิไซค์ที่เตรียมด้วยการแอลลอยด์เชิงกล. (EFFECTS OF COPPER ADDITION ON THERMOELECTRIC PROPERTIES OF β-FeSi$_2$ PREPARED BY MECHANICAL ALLOYING) อ.ที่ปรึกษา: ดร.สมชาย เกียรติกมลชัย, อ.ที่ปรึกษาร่วม: ดร.สิริพรรณ นิลไพรัช, 58 หน้า

สาร ไอรอนไดซิลิไซค์ถูกเตรียมด้วยเทคนิคการแอลลอยด์เชิงกลโดยใช้เครื่องบดเพลเนททารีบอล (planetary ball mill) $Fe_{30-x}Cu_xSi_{70}$ โดย x = 0, 1, 2 หรือ 5 ถูกเลือกแทนที่จะเป็น $Fe_{33.33}Si_{66.67}$เพื่อ หลีกเลี่ยงเฟสโลหะ ε-FeSi สารผสมหลังบดแต่ละสัดส่วนถูกขึ้นรูป 2 วิธี สำหรับวิธีแรกสารผสมถูกอัด แน่นโดยปราศจากความร้อนด้วยความดัน 345 เมกะปาสคาล จากนั้นเผาแอนนีลในเตาเผาในบรรยากาศ อาร์กอนที่อุณหภูมิ 1073 เคลวิน หรือ 1173 เคลวิน และใช้เวลาในการเผา 1 ชั่วโมง 3 ชั่วโมง หรือ 5 ชั่วโมง สำหรับวิธีที่สอง สารผสมถูกอัดแน่นพร้อมกับให้ความร้อนที่ความดัน 26 เมกะปาสคาล ด้วยอุณหภูมิ 1173 เคลวิน นาน 1 ชั่วโมง สารตัวอย่างถูกตรวจหาเฟสบีตา (β) ด้วยวิธีเลี้ยวเบนรังสีเอกซ์ (XRD) สัดส่วนของ เฟส β ต่อทุกเฟสในชิ้นสารและสัมประสิทธิ์ซีเบคเพิ่มขึ้นเมื่อเพิ่มทองแดงในสารที่เตรียมด้วยวิธีอัดแน่น โดยปราศจากความร้อน ค่าสัมประสิทธิ์ซีเบคที่สูงที่สุดในกลุ่มชิ้นสารที่เตรียมด้วยวิธีอัดแน่นโดยปราศจาก ความร้อนเป็นชิ้นสารตัวอย่างที่เจือด้วยทองแดง 0.5% และเผาแอนนีลที่อุณหภูมิ 1173 เคลวิน นาน 1 ชั่วโมง โดยให้ค่าสัมประสิทธิ์ซีเบค 16 μV/K ที่อุณหภูมิห้อง ชิ้นสารตัวอย่างที่เตรียมด้วยวิธีอัดแน่นพร้อม กับให้ความร้อนจะให้สัมประสิทธิ์ซีเบคสูงกว่าสัมประสิทธิ์ซีเบคของชิ้นสารตัวอย่างที่เตรียมด้วยวิธีอัด แน่นโดยปราศจากความร้อน ในกลุ่มชิ้นสารที่เตรียมด้วยวิธีอัดแน่นพร้อมกับให้ความร้อน สัดส่วนของเฟส β ต่อทุกเฟสในชิ้นสารและสัมประสิทธิ์ซีเบคจะมีค่าสูงที่สุดเมื่อเจือทองแดงประมาณ 0.1% - 0.2% ค่า สัมประสิทธิ์ซีเบคที่สูงที่สุดเป็นชิ้นสารที่เตรียมด้วยวิธีอัดแน่นพร้อมกับให้ความร้อนที่เจือด้วยทองแดง 0.1% โดยให้ค่าสัมประสิทธิ์ซีเบค 66 μV/K ที่อุณหภูมิห้อง

ภาควิชา ฟิสิกส์	ลายมือชื่อนิสิต
สาขาวิชา ฟิสิกส์	ลายมือชื่ออาจารย์ที่ปรึกษา
ปีการศึกษา 2549	ลายมือชื่ออาจารย์ที่ปรึกษาร่วม

PANUWAT ATTACHOTSAKDA: EFFECTS OF COPPER ADDITION ON THERMOELECTRIC PROPERTIES OF β-FeSi$_2$ PREPARED BY MECHANICAL ALLOYING. THESIS ADVISOR: SOMCHAI KIATGAMOLCHAI PH.D., THESIS COADVISOR: SIRIPAN NILPAIRACH PH.D. , 58 pp.

FeSi$_2$ were prepared by mechanical alloy (MA) technique using a planetary ball mill. Fe$_{30-x}$Cu$_x$Si$_{70}$ where x = 0, 1, 2 and 5 were selected instead of conventional composition, Fe$_{33.33}$Si$_{66.67}$, in order to avoid the metallic ε-FeSi phase. Each composition was solidified by 2 methods. For the first method, the mixtures were cold pressed with 345 MPa gauge pressure and annealed under Ar atmosphere at 1073K or 1173K. The annealing times were 1, 3 or 5 hours. For the second method, the mixtures were hot pressed with 26 MPa gauge pressure at 1173K and 1 hour soaking time. X-Ray Diffraction technique (XRD) was used to determine β phase of the samples. The β phase fraction and Seebeck coefficient of cold pressed samples increased when %Cu addition increased. Seebeck coefficient of cold pressed samples showed that 0.5%Cu sample annealing at 1173K for 1 hour gives the highest Seebeck coefficient of 16µV/K at room temperature. Seebeck coefficient of hot pressed samples was greater than that of cold pressed samples. For hot pressed samples, the β phase fraction and Seebeck coefficient is maximize with content of Cu around 0.1% - 0.2%. Seebeck coefficient of hot pressed samples showed that 0.1%Cu sample gives the highest Seebeck coefficient of 66µV/K at room temperature.

Department...........Physics.........   Student's signature.......................................

Field of study.........Physics..........   Advisor's signature............................

Academic year ....2006............   Co-advisor's signature.................................

Acknowledgements

Table of Contents

Table of Contents

List of Tables

List of Figures

Figure   **page**

CHAPTER I

INTRODUCTION AND LITERATURE REVIEW

1.1 Introduction

Nowadays, Thailand is facing the energy shortage problem. There are several renewable energy researches in Thailand especially in solar cell projects and fuel cell projects in order to relieve the long term problem. Solar cell is the device which can convert solar energy or photon energy into electrical energy. It is well known that solar cell cannot operate in cloudy day. Fuel cell can generate electrical current via electrochemical reaction by using methanol as substance. Certainly, methanol production must have some cost. There is the fact that Thailand has not yet used thermal energy which is abundant as much as possible. If thermal energy source such as geothermal, heat-waste from industry, solar etc. can be used as useful energy source, Thailand will get thermal energy sources as important and valuable renewable energy source. In order to use thermal energy conveniently in everyday life, the best way is conversion it into electrical energy which is the easiest to use. Thermoelectric effect which is discovered accidentally by Thomas Seebeck in 1969 is the physical phenomenon underlying the conversion of thermal energy into electrical energy directly by using thermal gradient.

The thermoelectric generator made from the junction between n-type and p-type semiconductors has advantages over the conventional turbine generator as the following:

- it is a compact system without mechanical devices;
- it is maintenance free;
- it has a long-term reliability and a long life time;
- it has an applicability to various heat source capacities and a flexibility to the fluctuation of heat input.

These advantages lead to a great potential in thermoelectric power generation for the recovery of waste heat in industrial processes and the use of renewable energy such as solar energy and ocean thermal energy. However, there are two main limitations consisting of low conversion efficiency and high cost. To make a thermoelectric generator practicable, further improvements in cost and conversion efficiency are needed [1].

There have been much effort to find the best thermoelectric materials [2-3] with numerous discussions of the physical limits. The efficiency of thermoelectric energy converters depends on the transport coefficients of the constituent materials through the figure of merit [2]:

$$Z = \frac{S^2 \sigma}{\kappa_{el} + \kappa_{ph}}, \qquad (1)$$

where σ is the electrical conductivity and S is the Seebeck coefficient. The quantities in the denominator are the thermal conductivities; it is given by the sum of contributions from the electronic carriers κ_{el} and the lattice κ_{ph}. The efficiency is increased by making ZT as large as possible, where T is the mean operating temperature of the device. At room temperature, the best thermoelectric material now known is Bi_2Te_3, which has $ZT \approx 1$ [2, 3]. With this value, the coefficient of performance of thermoelectric coolers is about one-third the value for conventional compressor systems. At room temperature, with the current design, thermoelectric refrigerators will be competitive with conventional compressor systems if a material with $ZT \approx 4$ is found. However, any small increment in this value ($ZT \geq 1$) will result in many new applications for these devices. This technology is environmentally cleaner and more reliable than traditional compressor systems. Therefore, it is worth exploring the possibility of increasing ZT to find a material with $ZT > 1$. No material is found at lower temperature with $ZT = 1$, although several are known at much higher temperatures: they are used in power generators.

From the definition of the figure of merit given in Equation (1), it is clear that, to increase Z, we have to decrease the thermal conductivity of the material and/or increase the thermopower and electrical conductivity. In order to the improvement in conversion efficiency, various studies have been mainly directed to the decrease in the thermal conductivity with the minimum effects on electrical conductivity and Seebeck coefficient.

The Weidmann-Franz law states that $\kappa_{el}/\sigma T = L_0 = 2.44 \times 10^8$ V^2/K^2.

Therefore the electronic contribution of the thermal conductivity is a constant (Lorenz number=L_0) at a given temperature. Although κ_{el} is proportional to $1/\rho$, in many semiconductors κ_{ph} is much greater than κ_{el}, so that one challenge is to minimize κ_{ph}

Metals are poor thermoelectric materials because they have a low Seebeck coefficient, and large electronic contribution to thermal conductivity, so electrical conductivity (σ) and thermal conductivity (κ) will cancel each other out. Insulators have a high Seebeck coefficient, and a small electronic contribution to thermal conductivity, however their charge density and electrical conductivity are low leading to a low thermoelectric effect. The best thermoelectric materials are between metals and insulators; i.e. semiconductors. In general, the best compromise seems to be to use heavily doped semiconductors to produce a carrier density of about 10^{19} cm^3. At this high carrier concentration κ_{ph} still accounts for more than 75% of the thermal conductivity.

The next step is finding semiconductors with a low lattice contribution to the thermal conductivity, thus maximizing the dimensionless figure of merit. One way to lowering κ_{ph} is to have heavy element in the unit cell. High atomic masses could reduce the atomic vibration frequencies and a large average coordination number per atom thus

Other approaches include having large number of atom (N) in the unit cell by using alloys to prepare structurally complex materials. The large N lowers the fraction of vibrational modes (phonons) that carry heat efficiently (the acoustic modes) to 1/N. The

disorder of random atomic substitution in an alloy scatters the phonons, lowering the mean free path which reduces the thermal conductivity.

In the last approach, preparing materials with a particular kind of structural complexity, these include the methods of employing grain refinement, fine inclusion dispersion, alloy disorder formation, etc.[4]. So that one or more component elements "rattle" in a cage made from a framework of other elements. The rattling vibrations lower the lattice thermal conductivity, hopefully without increasing the resistivity, because the carriers travel only in the framework. And also, phonon scattering at grain boundaries is significant in solid solutions. The electrical properties should be unaffected by grain boundary scattering down to grain sizes of ~ 0.1 µm, after which the grain size becomes comparable to the mean free path of the carriers in these alloys.

Various theoretical models have been used to predict the magnitude of the reduction in thermal conductivity with grain size. Good agreement between theory and experiment has been obtained for lightly doped materials [5, 6].

More direct relevance to the thermoelectric application is the effect of phonon-grain boundary scattering on the thermal conductivity of heavily doped alloys. In these materials phonon-grain boundary scattering is effectively in competition with phonon-carrier scattering; consequently the reduction of lattice thermal conductivity with grain size is expected to be less than in the undoped alloy. Although to date a completely satisfactory model of heavily doped fine-grained silicon-germanium alloy has proved elusive, it has been predicted that the lattice thermal conductivity would be reduce by 20 – 30% in material with a grain size of < 1µm [5]. As the electrical conductivity and Seebeck coefficient do not change with grain size, the thermoelectric figure of merit and conversion efficiency is substantially higher in fine-grained material compared to "single-crystal" [7]. In addition, the optimum carrier concentration decreases with a reduction in grain size [8].

To summarize, the features of a new semiconductor material with high ZT will likely be

1. a high symmetry crystal structure (high N_v) with a large number of heavy elements per unit cell (low κ_{ph}),

2. alloying or "rattling" to further reduce the lattice thermal conductivity,

3. the ability to dope the material to a high carrier density of about 10^{19} carrier/cm^3 (this generally gives optimal Z).

This list of needs remains daunting, because the structure of most new materials cannot be predicted. There are grounds for optimism that a ZT of 4 can be attained, but little basis for predicting when this occurs.

Bi_2Te_3 based alloys have been used for thermoelectric generator due to their excellent thermoelectric properties. However, the tellurium, Te, is very high cost and the tellurium reserve is not abundant. Te resources will easily be depleted by the increase in demand to provide massive amounts of Bi_2Te_3-based alloys as thermoelectric materials in large scale thermoelectric generator. In addition, most tellurium compounds are harmful to the human body. Serious environmental pollution may be caused without a proper method for recycling. Further more, these materials are expensive and often mechanically weak and generally require protection against oxidation and vaporization. Nevertheless, there are some tasks where low performance of thermoelectric generators is not an obstacle, but the best thermoelectric materials contain tellurium that is one of the rarest elements on the Earth. The average contents of tellurium in Earth crust is about 1×10^{-7}% mass. So, it is practically impossible to provide every car by thermoelectric generator using waste heat because of shortage of tellurium. Therefore, Bi_2Te_3-based alloys are not considered to be suitable materials for large scale thermoelectric generator.

Material availability is one of the most important factors when we consider the mass-production of next generation thermoelectric devices. The abundant elements which at least for 100-200 years will not face the shortage of supply are Si, Fe, Ca and Ba [9].

In recent years, iron disilicides, β-FeSi$_2$, have received great attention due to their low cost, availability (composed of the two most abundant), non-toxic, good resistant against oxidation, chemical stability and the possibility of improved thermoelectric efficiency [10-19]. These advantages create great potential for commercial use. And β-FeSi2 has also received considerable attention as an attractive material for optoelectronic and photovoltaic applications [20]. Therefore, semiconducting iron disilicide, b-FeSi2 , is one of the potential candidates for practical use in the high temperature range up to 1200 K [11, 21, 22].

However, the iron disilicide produced by conventional ingot technology is usually composed of tetragonal α-Fe$_2$Si$_5$ and cubic ε-FeSi [10, 23-25]. These phases which are metallic phase can not be engaged in thermoelectric application. Annealing is involved in β-FeSi$_2$ preparation process in evitable to induce the peritectoid reaction from α and ε phase to β phase and the eutectoid decomposition from α phase to Si and β phase.

The p- and n-type semiconductors used for thermoelectric generators should be simple and energy saving in their fabrication process. These options can be achieved by a powder metallurgy processing. When fabricating porous iron disilicide based p- and n-type compounds by a powder metallurgy, it is expected that the figure of merit can be strongly enhanced by reducing thermal conductivity without any significant losses in the electrical conductivity and Seebeck coefficient [26, 27]. It was also reported that the maximum power output increase with increasing porosity [28].

The main features of β-phase iron disilicide material are as follows:
1. Both P-type and N-type semiconductor are easily obtained by adding manganese or cobalt respectively, and they are defined Fe$_{1-x}$Mn$_x$Si$_2$ and Fe$_{1-y}$Co$_y$Si$_2$ by chemical formula.
2. Both materials are simply fabricated by the powder metallurgical technique which is considered to have fundamentally low cost feasibility in quantitative production.
3. Low purity (98%) industrial grade raw materials are sufficient in quality and this makes a basically low cost device possible.

4. Raw materials used are plentiful in resources: iron, silicon, manganese and small amount of cobalt as an additive.

5. They pose no health hazard and produce no hazardous waste.

6. They withstand high temperature up to 1123K and so make direct thermoelectric conversion from flames possible.

The β-Fesi2 can be produced by the Mechanical Alloying, MA, [29-32] in a much simpler way than by conventional melt and cast processes as is shown in Figure 1-1.
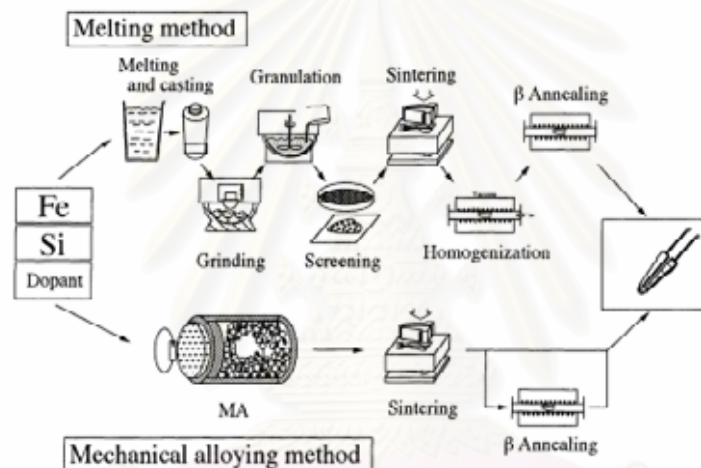
Figure 1-1: Schematic illustrations showing the two ways of the formation of FeSi$_2$ thermoelectric generator [32].

Mechanical Alloying is a solid state alloying process by using ball mill [4]. Mechanical alloying (MA) was originally introduced as a means of producing fine and uniform dispersion of oxides in super alloy matrix [33]. At present it is widely applied for the synthesis of a variety of materials, for example, nanocrystalline, amorphous, non-equilibrium, composite metal powders, etc.[34] MA is ideally suitable for the synthesis of those materials whose properties can be improved by grain refinement and dispersion of a second phase. So, MA materials having a fine grain size can improve thermoelectric conversion efficiency by the reduction in lattice thermal conductivity [4, 29, 31, 32, 35].

Consequently, powders compacting $FeSi_2$ has good thermoelectric properties as compared with conventional monocrystalline thermoelectric.

β-$FeSi_2$ compounds with densities close to the theoretical density have been synthesized by sintering under applied pressure, i.e., hot-press or SPS (Spark Plasma Sintering) etc.[36, 37]. However, for practical use, it is desirable that the compounds should be manufactured by pressureless sintering rather than by hot-pressing or SPS in terms of production costs and productivity. The synthesis of β-$FeSi_2$ by pressureless sintering generally necessitates the sintering at high temperature and heat treatment at 970-1220K for a long time in order to obtain a densely sintered body of β-$FeSi_2$. If the sintering process can be simplified, it is expected that this simplicity will lead to the further reduction of β-FeSi2 production costs compared to the conventional method.

1.2 Literature Review

Umemoto (1995) [32] prepared β-$FeSi_2$ doped with Al and Mn by mechanical alloying using horizontal ball mill. Powders of elements Fe(>99.9% purity, <150µm), Si(>99.9% purity, <10µm), Mn(>99.9% purity, <75µm) and Al(>99.9% purity, <180µm) were used as starting materials. MA powders of the composition $Fe_{30}Si_{70}$ milled for various times were examined by XRD. It was reported that the appropriate milling time was consider to be about 200 hours where the size is very fine at around 1 µm. The phase transformation in the MA powder milled for 200 hours by heat treatment was examined using cold compacted specimens made of various compositions of MA powders. Specimens were heated to various temperatures and kept for 10 minutes and air cooled. The results indicated that a little increasing in Fe content in MA powders shifts the ε phase formation range slightly to the Si-rich side. β, $\beta+\alpha$ and $\alpha+\varepsilon$ phases are seen in the specimens of $Fe_{30}Si_{70}$ heated to 1173K, 1223K and 1273K, respectively. These results well corresponds to the phase diagram. Then, the transition rate from $\alpha+\varepsilon$ to β phase was examined using the cold compacted MA powders with composition $Fe_{30}Si_{70}$ milled for

200 hours. Compacted specimens were initially heated at 1273K for 10 minute to produce $\alpha+\varepsilon$ structure and annealed at various temperatures between 873K and 1173K for 60 minutes in vacuum to transform to β phase. It was found that the volume fraction of β phase has two maxima at around 1153K and 1000K. Next, The 200 hours milled MA powders of $Fe_{28}Mn_2Si_{67}Al_3$ were hot press sintered at 1353K for 30 minutes under a pressure of 36 MPa into a disk of 60 mm diameter followed by annealing at 1033K for 100 hours to transform to β phase. Thermoelectric properties were measured. It was concluded that the specimens prepared by hot press sintering from MA powder showed higher figure of merit and higher conversion efficiency than that prepared by conventional ingot metallurgy. The improvement is mostly due to the lower thermal conductivity associated with the fine grain size produced by MA. The paper was also reported that the transformation rate from $(\alpha + \varepsilon)$ to β in the MA powder is faster than that in the specimen prepared by conventional ingot metallurgy. In publication of Umemoto, the milling time was quite so long because they chose horizontal ball mill which is suitable for industry. If the β-$FeSi_2$ is prepared by using planetary ball mill which is appropriate for laboratory work, the milling time must less than that of horizontal ball mill due to the high impact energy and high impact frequency of planetary ball mill.

Min et al. (1998) [30] prepared Co-doped n-type iron disilicides by MA. Reagent grade powders (>99.9% purity) less than 150 μm in particle diameters were used as the starting materials in the mechanical alloying process. The powders contain more Si than the stochiometric composition in order to achieve dispersion of Si phase; that is, in the formula of $(Fe_{0.95}Co_{0.05})_xSi_2$. Two value of x (0.9 and 0.8) were chosen. It was found that 50 hours of milling was sufficient to get FeSi compound with the grain size of approximately 1.2 μm. Sintering was accomplished by the pressure-resistance-sintering device with five temperature variance in the range of 760-880°C at pressure of 50 MPa. The results showed that ε-FeSi phase remained untransformed within the matrix of β-$FeSi_2$ and Si phases when sintered at the temperature lower than 790°C. The paper was concluded that increasing of sintering temperature, mean sizes and interspacing of Si phases slowly increase and rapidly increase, respectively. Furthermore, the mobility

varied significantly with the changes in interspacing and the volume fraction of Si phases. While the change in carrier concentrations was smaller than that of the mobility, lead to increasing of electrical conductivity. Moreover, Seebeck coefficient -183±2 µV/K was obtained regardless of changes in the sintering temperatures and compositions. The thermal conductivity decreased with the interspacing of Si phases. A slight improvement of Z value was attributed to the effective phonon scattering by the finely dispersed Si phase in the β-FeSi$_2$ matrix. That paper implied that heat treatment temperature should be kept at low but enough to obtain β-FeSi$_2$ formation in order to improve the figure of merit.

Ur et al. (2002) [31] prepared n-type FeSi$_2$ doped with Co by MA using high energy attrition milling. Powder mixtures of -325 mesh Fe (>99.9%), -200 mesh Si(>99.9%), and -200 mesh Co(>99.9%) designed to yield Fe0.98Co0.02Si2 were mechanical alloyed for 120 hours under an Ar atmosphere. As-sieved powder size was typically from 3 to 6 µm, and the morphology was generally spherical. After degassing in vacuum at 400°C for 2 hours, powders were hot pressed using graphite. The hot pressing operation was carried out under vacuum with a pressure of 35 MPa at 1000°C for 2 hours and 60 MPa at 1100°C for 4 hours. In order to investigate the degree of alloy during milling, consolidation and isothermal annealing, XRD analysis was carried out for MA powders and as-consolidated specimens. In order to observe microstructures and identify phases, SEM/EDX was employed. Microhardness was measured to characterize general mechanical properties. The XRD patterns showed that the elemental Si peak disappeared after 72 hours of milling. The MA powders were believed to be in a metastable state presumably due to the inherently slow rate of phase transformation, which led to processing for at least 500 hours of milling to induce β-FeSi$_2$ formation by MA. Thus it was considered that phase transformation proceeds further if a proper post-annealing is applied to the metastable phase powder. Next, the powders were successfully consolidated by vacuum hot pressing, VHP. Near fully at 1100°C and 60 Mpa for 4 hours. The high density compact is shown to consist of the untransformed mixture of α -Fe$_2$Si$_5$ and ϵ-FeSi. The XRD analysis after the isothermal annealing at 830°C for 4-96 hours revealed that progressive β-FeSi$_2$ transformation from α -Fe$_2$Si$_5$ and ϵ-FeSi took place

along with the annealing times. However, a small portion of untransformation metallic phases of α and ε still remained even after 96 hours of annealing due to their inherent sluggish peritectoid reaction. The full transformation annealing time was approximated about few hundred hours from the principal peak square ratio, $[I_{\alpha}/I_{\beta}]^2$. Because the slope of $[I_{\alpha}/I_{\beta}]^2$ is shown to be dulled at around 24 hours and the microhardness saturation is shown after 12 hours of annealing, they suggested that the effective and economical way to produce β-FeSi$_2$ transformation is approximately 24 hours annealing at 830°C after vacuum hot pressing(VHP) at 1100°C under 60 MPa for 4 hours.

Another important process of β-FeSi$_2$ preparation is annealing process. The speed of such a peritectic reaction from metastable tetragonal $\alpha + \varepsilon$ phase to β phase is consider to be extremely low [10, 11, 12, 16, 23, 25, 31, 32, 38-40]. To obtain β-FeSi$_2$ by annealing the α-FeSi$_2$ sample about 10 x 1 x 1 mm^3 which prepared by the Czochralski technique, need to annealed at 800C for 240 h. [16]. Due to large of annealing time, there are a few groups of researcher studying the way to decrease the annealing time.

Yamauchi et al. (1997a) [23] prepared the various binary FeSi$_2$-(Mn,Co) alloys with a addition of Cu (0.1, 0.2, 0.5,and 1.0 at.%) from 99.9mass% electrolytic iron, high purity Si used commonly as semiconductors, 99.9mass% electrolytic Cu, Mn and Co. The elements were melted in an alumina crucible under an Ar gas atmosphere. The molten metal was cast into a quartz tube of 4 mm in inner diameter by a vacuum suction method. As-solidified and annealed at 1073K, the structures were examined by BEI (back scattered electron image) of SEM without etching. The transformation behavior was examined by micro thermal differential analysis (DTA) and by XRD using a Cu target. The thermoelectric power was measured at 373K by using a temperature difference of about 25K between the hot and cold ends. The results show that the addition of 0.2 at.% Cu was the most effective on β formation. The β formation rate in the Cu added alloys was more than 100 times higher than in the Cu free alloys. Furthermore, the maximum thermoelectric power of the lower Cu alloys was higher than that of higher Cu alloys. It was concluded that the lower maximum thermoelectric power in the alloy of higher Cu content may be that Cu decreases the effect of the dopant. The maximum Seebeck

coefficient value of the $Fe_{27.86}Si_{71.04}Mn_{1.0}Cu_{0.1}$ alloy was about 400 $\mu V/K$, which is remarkably higher than the 290 $\mu V/K$ reach in the conventional cast $Fe_{0.9}Mn_{0.1}Si_2$ alloy annealed at 1073K for 8.6×10^3s. The thermoelectric power was almost the same in the n-type material doped with Co. The maximum value was about -200 $\mu V/K$, which is slightly larger than the -170 $\mu V/K$ reached in the conventional $Fe_{0.9}Co_{0.1}Si_2$ alloy annealed for 8.6×10^4s.

Yamauchi et al. (1999b) [39] prepared Cu added iron disilicide alloys. The alloys were prepared from 99.9 mass% electrolytic iron, high purity Si, 99.9 mass% electrolytic Mn and Cu. These elements were melted in an aluminum crucible under Ar atmosphere. The molten metal was cast into a quartz tube of 4 mm in diameter by a vacuum suction method. The heat treatment for β-phase was carried out at various temperatures below 1210K. The results showed that in the Cu free alloy doped with 1 at.% Mn, the time for complete β phase formation was more than 10^6 s when annealing at 873 K. On the other hand, in the Cu added alloy, it was only about 8×10^3 s at 873 K. In addition, they suggested the annealing at 873 K of the Cu added alloy can be applied commercially because the time is two order shorter than that in the Cu free alloy. The paper was concluded that the shape of the Si dispersoids formed by the eutectoid decomposition changed from lamellar in the Cu free alloy to granular in the Cu added alloy. In the FeSi2 alloy, the peritectoid reaction ($\alpha + \varepsilon \rightarrow \beta$) was also enhanced by the addition of Cu. And the size of Si dispersoids was very fine when heating below 1023 K.

Yamauchi et al. (2002c) [40] prepared iron disilicide alloys with a small amount of Pd, Pt, Cu, Ag and Au. Various $Fe_{29.4}Si_{70.5}X_{0.2}$ and $Fe_{28.5}Si_{70.5}X_{1.0}$ (X = Au, Ag, Cu, Pd, Pt) alloys were used. These alloy were prepared from 99.9 mass% electrolytic iron, high purity Si. The purity of the additional element was a regular grade (99.9% up). These materials were melted in an alumina crucible under Ar atmosphere. The molten metal was cast into a quartz tube of 3 mm in diameter by a vacuum suction method. The Isothermal heat treatment for the β phase was carried out at 1073 K which is a temperature between the eutectic temperature of PdSi-Si eutectic (1143 K) and the Au-Si

eutectic (636 K). The paper was concluded that a small amount of Au and Pd was effective in accelerating the eutectoid decomposition ($\alpha + \varepsilon \rightarrow \beta$) though the effect is slightly lower than that of Cu addition. In a 0.2 at.% Pd containing alloy annealed for 600 s, finely lamellar and homogeneous eutectoid structure were observed. In a 0.2 at.% Au containing alloy annealed for 6×10^2 s, the structure was quite inhomogeneous. A similar result was obtained in a 0.2 at.% Cu containing alloy. In addition, the solubility of Cu, Au and Pd in β phase was beyond 0.2 at.% and higher than in the α phase. On the other hand, in the case of Ag and Pt, the solubility of them in the β phase was negligibly small.

Kim et al. (2003) [25] prepared Cr doped p-type and Co doped n-type β-FeSi$_2$ alloys by using a powder metallurgy technique. In this work, the addition of 0.5 at.% Cu is to enhance the α to β phase transformation. The raw materials were Fe powder (99.9% pure), Si chip (99.9999% pure), Cr chip (99.99% pure), Co chip (99.99% pure),and Cu chip (99.5% pure). The alloys were arc-melted and crushed into fine flakes. The flakes were sieved to prepare powder whose diameter was under 45 μm. To optimize the sintering condition, the sieved powders were compacted at 673K under 625 Mpa and 656 Mpa, respectively. The specimens are sintered at temperature from 1403K to 1473K for 3 hours under vacuum. In order to obtain the semiconducting β-FeSi$_2$ phase, all sintered specimens were heat-treated at 1113K for 10 hours in a sealed quartz tube under vacuum. Phase constitution and microstructure were characterized by XRD and SEM-EDS. The results show that the optimum condition was selected as sintering at 1463K for 3 hours after compacting under 656 Mpa at 673K. However, there are some ε-FeSi phase remaining in specimens after annealing at 1113K for 10 hours. They suggested that the presence of the ε-FeSi could come from a deficiency of Si due to the oxidation during powder preparation. Then, the thermoelectric properties were analyzed by measuring of thermoelectric powder, electrical conductivity and thermal conductivity. The thermoelectric power and the electrical conductivity were simultaneously measured in a temperature range from 373K to 973K in a He atmosphere. The Seebeck voltage was measured upon applying a small temperature difference, ΔT (1, 3 and 5K) between both

ends of the specimens. A sub-heater was attached to one of the Ni blocks to provide a temperature difference. Thermoelectric power was determined by using the least square method. The electrical conductivity was measured using DC four-probe technique. The thermal conductivity was calculated by the laser flash method using the thermal constant analyzer (ULVAC TC-7000) in a temperature range from 373K to973K under vacuum. From the results, the figure of merit of binary β-FeSi$_2$ is 0.19×10^{-4}K^{-1}. It was found that figure of merit increase by the addition of Cr and Co. However, the figure of merit of Cu doped β-FeSi$_2$ is slightly decreases. The maximum figure of merit was found to be 1.3×10^{-4}K^{-1} in Fe$_{0.95}$Co$_{0.05}$Si$_2$ at 657K.

It can be implied from this work that the powders should contain more Si than the stoichiometric composition in order to avoid appearance of ε-FeSi phase. Furthermore, the slightly decreasing of figure of merit of Cu doped β-FeSi$_2$ may be the effect of a high addition of Cu (0.5 at.%). The publication of Yamauchi (1997a) [14] indicated that a high addition of Cu decreases the effect of the dopant.

In this thesis, β-FeSi$_2$ will be prepared by MA using the planetary ball mill. The thermoelectric properties of the material which is prepared by mechanical alloying technique should be improved. The milling time can be reduced by using planetary ball mill because of its high impact energy and high impact frequency. The composition of Fe$_{30}$Si$_{70}$ was chosen in stead of conventional composition in order to avoid the metallic ε-FeSi phase. The small addition of Cu was added in order to decrease annealing time.

CHAPTER II

THEORY

2.1 Thermoelectric Effect

The thermoelectric effect is the phenomenon underlying the conversion of thermal energy into electrical energy. Its physical significance can be appreciated by considering the effect of imposing a steady temperature gradient along a finite conductor. Initially the conductor possesses a uniform distribution of charge carriers, but in the presence of a temperature gradient the free carriers at the hot end will have a greater kinetic energy than that of cold end and tend to diffuse to the cold end. The build up of charge results in voltage. The open circuit voltage when no current flow is the Seebeck voltage. In addition, the induced voltage between the ends of the conductor depends only on the temperatures of the ends. Whatever the distribution of temperatures, the same voltage will appear between the ends [29].

A thermoelectric device consists of a number of alternate n- and p-type semiconductor thermoelements, which are connected electrically in series by metal interconnects, in order to gain the voltage. They are sandwiched between electrically insulating but thermally conducting ceramic plates to form a module. When a temperature difference is maintained across the module, electrical power will be delivered to an external load.

A thermoelectric device should have a high value of figure of merit, Z, which represents the efficiency of thermoelectric materials. The figure of merit is given by

$$Z = \frac{S^2 \sigma}{\kappa} \quad , \quad (2)$$

where S is Seebeck coefficient, σ is electrical conductivity, κ is thermal conductivity. Therefore, the thermoelectric material needs to have high Seebeck coefficient, high electrical conductivity and low thermal conductivity.

In Seebeck effect, the temperature difference between two points in a conductor or semiconductor results in a voltage difference between these two points. Stated differently, a temperature gradient in a conductor or a semiconductor gives rise to a built-in electric field. This phenomenon is called the Seebeck effect or the thermoelectric effect. The Seebeck coefficient gauges the magnitude of this effect. The thermoelectric voltage developed per unit temperature difference in a conductor is called the Seebeck coefficient. Only the net Seebeck voltage difference between different metals can be measured. The principle of the thermocouple is based on the Seebeck effect

Consider an aluminum rod that is heated at one end and cooled at the other end as depicted in Figure 2-1. The electrons in the hot region are more energetic and therefore have greater velocities than those in the cold region. Consequently, there is a net diffusion of electrons from the hot end toward the cold end which leaves behind exposed positive metal ions in the hot region and accumulates electrons in the cold region. This situation prevails until the electric filed developed between the positive ions in the hot region and the excess electrons in the cold region prevents further electron motion from the hot to cold end. A voltage is therefore developed between the hot and cold ends with the hot end at positive potential. The potential difference ΔV across a piece of metal due to a temperature difference ΔT is called the Seebeck effect. To gauge the magnitude of this effect we introduce a special coefficient which is defined as the potential difference developed per unit temperature difference, i.e.

$$S = \frac{dV}{dT},$$

(3)
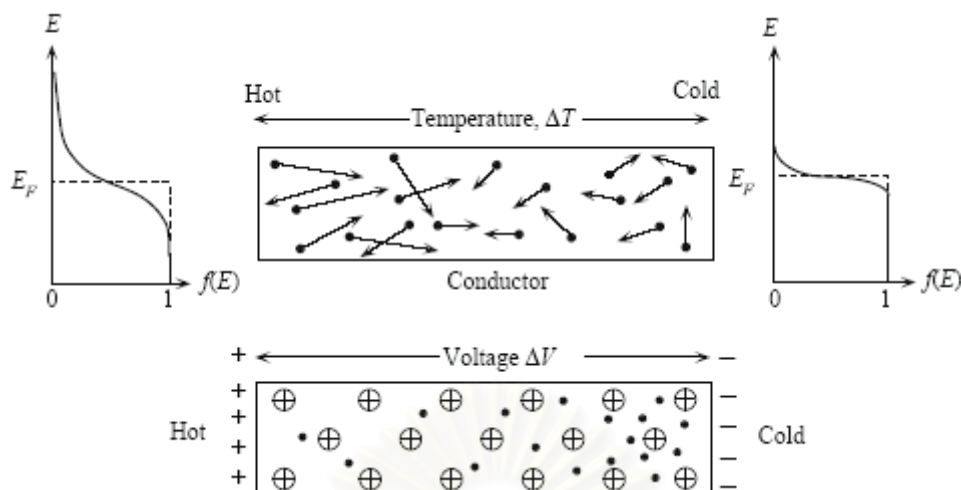
Figure 2-1: A temperature gradient along a conductor gives rise to a potential difference [3].

By convention, the sign of S represents the potential of the cold side with respect to the hot side. If electrons diffuse from hot to cold end, then the cold side is negative with respect to the hot side and the Seebeck coefficient is negative. In a p-type semiconductor, on the other hand, holes would diffuse from the hot to cold end. The cold side would be positive with respect to the hot side which would make S a positive quantity.

S is a material property that depends on temperature; $S = S(T)$. It is tabulated for many materials as a function of temperature. Given the Seebeck coefficient $S(T)$ for a material, the voltage difference between two points where temperatures are T_0 and T, from equation 1, is given by

$$\Delta V = \int_{T_0}^{T} S dT \quad , \qquad (4)$$

The voltage difference in equation 4 above is for the cold end with respect to hot as in the convention for S.

Charge carriers in the materials (electrons in metals, electrons and holes in semiconductors, ions in ionic conductors) will diffuse when one end of a conductor is at a different temperature than the other. Hot carriers diffuse from the hot end to the

cold end, since there is a lower density of hot carriers at the cold end of the conductor. Cold carriers diffuse from the cold end to the hot end for the same reason. If the conductor were left to reach equilibrium, this process would result in heat being distributed evenly throughout the conductor. The movement of heat (in the form of hot charge carriers) from one end to the other is called a heat current. As charge carriers are moving, it is also an electrical current. In a system where both ends are kept at a constant temperature relative to each other (a constant heat current flows from one end to the other), there is a constant diffusion of carriers. If the rate of diffusion of hot and cold carriers in opposite directions were equal, there would be no net change in charge. However, the diffusing charges are scattered by impurities, imperfections, and lattice vibrations (phonons). If the scattering is energy dependent, the hot and cold carriers will diffuse at different rates. This creates a higher density of carriers at one end of the material, and the distance between the positive and negative charges produces a potential difference; an electrostatic voltage. This electric field, however, opposes the uneven scattering of carriers, and equilibrium is reached where the net number of carriers diffusing in one direction is canceled by the net number of carriers moving in the opposite direction from the electrostatic field. This means the thermopower of a material depends greatly on impurities, imperfections, and structural changes (which often vary themselves with temperature and electric field), and the thermopower of a material is a collection of many different effects.

The thermoelectric performance of semiconductors is evaluated by Z related to three physical properties of Seebeck coefficient α, resistivity ρ and thermal conductivity κ. These properties are given as a function of the carrier concentration and each property can not be controlled independently. However, thermal conductivity in heavily doped semiconductor is mainly due to the electric contribution κ_{el} and lattice contribution κ_{ph}[3, 41, 42]. Then, thermal conductivity is given by

$$\kappa = \kappa_{el} + \kappa_{ph} \quad , \qquad (5)$$

The thermal vibrations of the lattice are quantized and the quanta (phonons) migrate along the temperature gradient. Then a thermal current is generated as the result. The phonons are scattered and the thermal current is disturbed by collision among phonons, disorder in the lattice, and boundaries. The scattering is effectively caused when the wave length of the phonon is the same as the length between

disorders. Then phonon with higher energy are effectively scattered by disorder in the lattice and phonons with lower energy are scattered by grain boundaries.

In many solid solution systems, the scattering due to disorder caused by alloying reduces κ_{ph} by almost one order of magnitude. Therefore, the Z of a solid solution or an alloy is higher than that of a single compound or an element because of the reduction effect of κ_{ph} due to the phonon scattering with a higher energy [43].

On the other hand, the grain boundaries scatter phonons with a lower energy remarkably. The reduction effect of κ_{ph} by the boundary scattering occurs in a polycrystal with fine grains and the sintered materials [3, 42-44].

2.2 Phase Transformation

The crystallization kinetics is usually interpreted in terms of the standard nucleation-growth model formulated by Johnson-Mehl-Avrami (JMA). This model which describes the time dependence of the fractional extent of reaction phase is $1 - \exp[-(kt)^n]$, where the rate constant k is a function of temperature and in general depends on both the nucleation frequency and the crystal growth rate, and the kinetic exponent n is a parameter which reflects the nucleation frequency and/or the growth morphology.

2.3 Iron Disilicide

The iron-silicon phase diagram has been the subject of controversial considerations for a long time [45]. According to a generally accepted, summarized study [45], iron and silicon form five compounds consisting of Fe_2Si, Fe_5Si_3, ε-$FeSi$, α-Fe_2Si_5 and β-$FeSi_2$.

In the Fe-Si system, there are three considered phases consisting of α-Fe$_2$Si$_5$ phase, ε-FeSi phase and β-FeSi$_2$. Tetragonal α-Fe$_2$Si$_5$ phase is thermodynamically meta-stable at ambient temperature, while cubic ε-FeSi phase and tetragonal β-FeSi$_2$ phase are thermodynamically stable at room temperature. The phase diagram of Fe-Si system is shown in Figure 2-2.
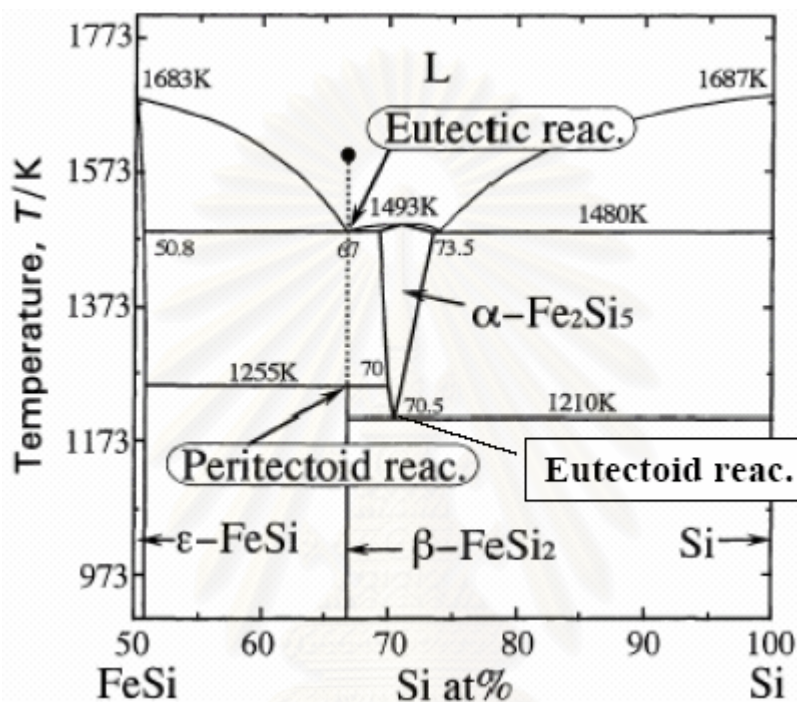
Figure 2-2: Phase diagram of Fe-Si system [46].

The equilibrium phase diagram [46] shows that the alloy with the stoichiometric composition of FeSi$_2$ solidifies at 1493 K as a eutectic composed of the tetragonal α and cubic ε phases. However, these high temperature phases are metallic and do not show high thermoelectric power. β-FeSi$_2$ is a stable semiconductor phase which could be formed by two kinds of mechanisms, following these:

1. Peritectoid reaction at 1255 K. The α-FeSi$_2$ phase + ε-FeSi phase transform into β–FeSi$_2$ phase. However, the kinetics of the peritectoid reaction is usually slow and it takes a long time to complete the reaction.

2. Eutectoid reaction at 1210 K. The α–Fe$_2$Si$_5$ phase transforms into the β–FeSi$_2$ + Si phases and subsequent Si phase + ε-FeSi transform into β below 1210K. However, α–Fe$_2$Si$_5$ does not easily undergo a transition to the low temperature phase β-FeSi$_2$.

In summary, α-Fe$_2$Si$_5$ phase and ε-FeSi phase which are metallic phases with poor thermoelectric properties can be transformed into β-FeSi$_2$ phase very slowly by heat treatment. Regarding to the phase diagram, the semi-conducting β–FeSi$_2$ phase is expected to be used as a high-temperature thermoelectric material [11, 47].

The crystal structures of α-Fe$_2$Si$_5$, ε-FeSi and β-FeSi$_2$ are shown in Figure 2-3.
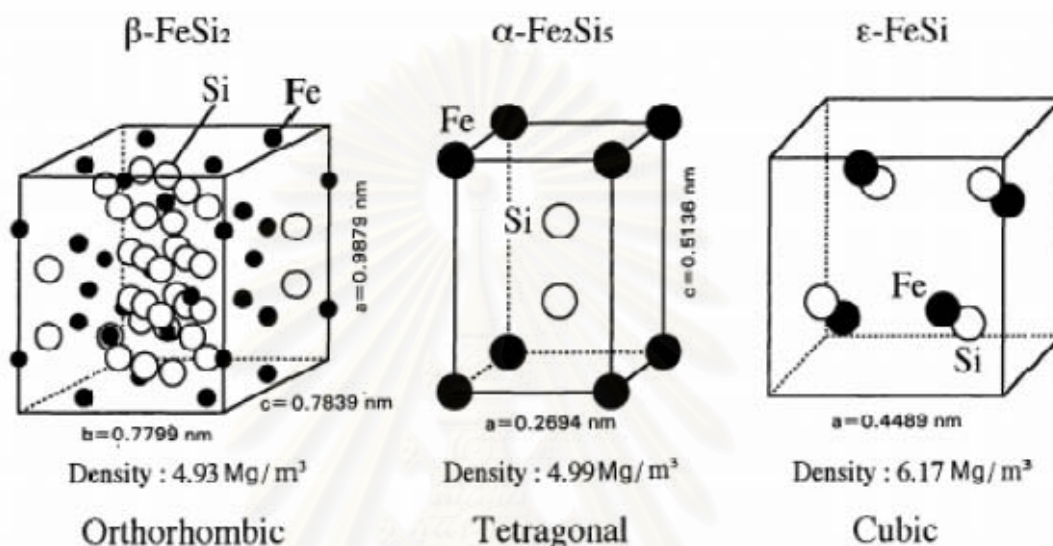
Figure 2-3: Crystal structures of β-FeSi$_2$, α-Fe$_2$Si$_5$ and ε-FeSi [32].

Metallic ε-FeSi has a cubic structure with 8 atoms in a unit cell, metallic α-Fe$_2$Si$_5$ has a tetragonal structure with 2.87 atoms in a unit cell and semi-conducting β-FeSi$_2$ presents an orthorhombic structure with 48 atoms in a unit cell [32].

The unit cell of the β-FeSi$_2$ phase consists of the 16 iron atoms and 32 silicon atoms as shown in Figures 2-3 and 2-4. The crystal structure is orthorhombic with a = 0.9879 nm, b = 0.7799 nm, c = 0.7839 nm. [32, 48]

Figure 2-4: Schematic stacking sequence of planes perpendicular to the *a*-axis in a unit cell of the β-FeSi$_2$ [49].

Normally, the β phase is an intrinsic semiconductor. There are possibilities to obtain both p-type and n-type of β-FeSi$_2$. The replacement of iron by an element to its left in the periodic table, e.g. Mn, Cr or other elements from this group, produces p-type semiconductor and right in the periodic table, e.g. Co, Ni or other ele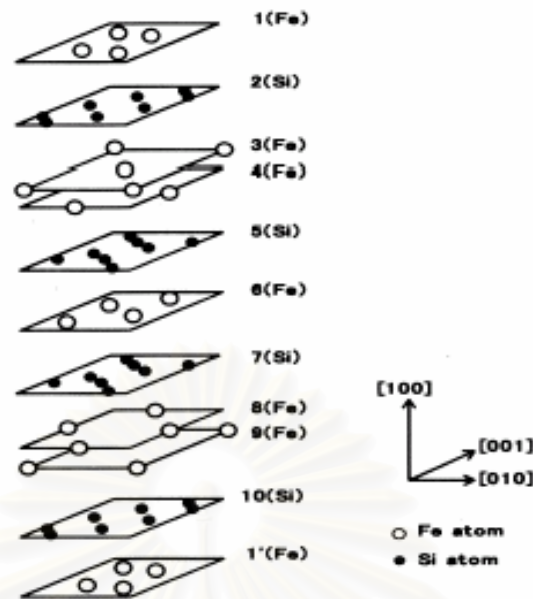ments from this group, produces n-type semiconductor. In addition, substitution of a group 3 element for silicon produces p-type semiconductor.

The doping of various elements such as Co, Cr, Ni, Mn, Al, Cu, B, Nb, and Zr are substituted for Fe. While Al was report to substitute for Si [50]. The addition of a small amount of Cu drastically increased the β –FeSi$_2$ phase transformation rate [39, 51].

2.4 Mechanical Alloying

Mechanical alloying, MA, is a ball milling process where a powder mixture placed in the ball mill is subjected to high energy collision from the balls. Mechanical alloying has been proved to be an advantageous method for the synthesis of

semiconducting thermoelectric compounds or solid solutions [52, 53]. The process is usually carried out in an inert atmosphere. It is an alternative technique for producing metallic and ceramic powder particles through the solid state reaction. The two most important events involved in mechanical alloying are the repeated welding and fracturing of the powder mixture. Since mechanical alloying is a solid state process, it provides a means to overcome the drawback of formation of new alloys using a starting mixture of low and high melting temperature elements.

The resulting powder material appears to be very homogeneous due to the large amount of induced grain boundaries. Although in general, the raw materials used in mechanical alloying should include at least one fairly ductile metal to act as a host or binder to hold together the other ingredients, a lot of studies have confirmed that brittle metals can also be mechanically alloyed to from solid solution, intermetalics and amorphous alloys as well.

There are several types of ball mill for mechanical alloying process such as attritor ball mill, planetary ball mill, horizontal ball mill, etc. Formation of composites in horizontal ball mill took an exceptional long time because the ball mill has limit energy. For an economical production of MA thermoelectric materials, a milling equipment with a high output rate is needed. From the available types of high energy ball mills, we have chosen the planetary type, since it principally allows an up scaling of the mechanics and a transfer of the derived laboratory results to larger systems.

Planetary ball mill is a very often used machine for mechanical alloying. Because very small amount of powder is required, the machine is suitable for research purpose in the laboratory. The ball mill consists of one turn disc (sometimes called turn table) and two or four bowls which are used to contain the powder and balls are on the disc. The turn disc rotates in one direction while the bowls rotate in the opposite direction. The centrifugal force created by the rotation of the bowl around its own axis together with the rotation of the turn disc is applied to the powder mixture and milling balls in the bowl. The powder mixture is fractured and cold welded under high energy impact.

Since the directions of rotation of the bowl and turn disc opposing, the centrifugal forces are alternately synchronized. Thus friction resulted from the milling balls and the powder mixture being ground alternately rolling on the inner wall of the bowl, and impact results when they are lifted and thrown across the bowl to strike at

the opposite wall. He impact is intensified when the ball strike one another. The impact energy of the milling ball in the normal direction attains a value of up to 40 times higher than that due to gravitational acceleration. The impact energy of the milling balls is changeable by altering the rotational speed of the turn disc. The advantage of this type of ball mill is not only that high impact energy could be obtained but also high impact frequency which can shorten the duration of the mechanical alloying process. However, the temperature of bowl may reach about 393K within a short milling duration of only 30 to 60 minute because of high impact frequency.

In a high energy mill, the particles of the metal powder are repeatedly flattened, fractured and re-welded. Every time two steel balls collide, they trap powder particle between them. The force of the impact deforms the particles and creates atomically clean new surfaces. When the clean surface comes in contact, they weld together. Since such surface readily oxidizes, the milling operation is conducted in an atmosphere of nitrogen or an inert gas.

At early stages in the process, the metal powders are still rather soft and the tendency for them to weld together into large particles predominates. Some particles have two to three times larger in diameter (10 times large in volume) than the original ones. As the process continues, the particles get harder. And their ability to withstand deformation without fracturing decreases. The larger particles are more likely to break apart when they are struck by the steel balls. In time, the tendency to weld and the tendency to fracture come into balance and the size of the particles becomes constant within a narrow range.

Although there is little change in the size of the particles after balance between welding and fracturing is attained, the structure of particles is steadily refined. The thickness of each layer in composite particles decreases because of the repeated of the steel balls. And the number of layers within each particle increases. The rate of refinement of the internal structure of particles is roughly logarithmic with processing time.
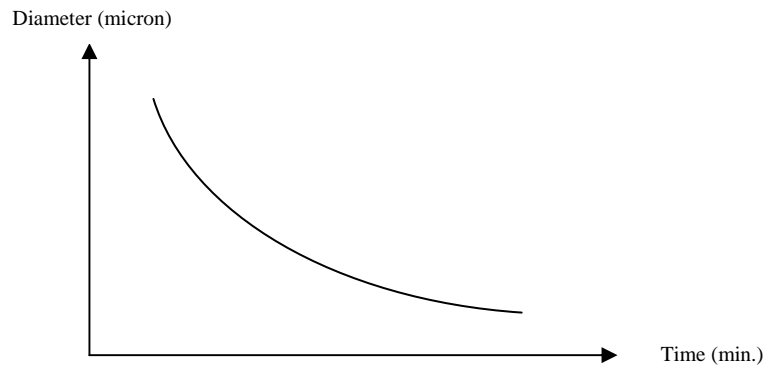
Figure 2-5: Rate of refinement of particles. It is roughly logarithmic with processing time.

There is a slight tendency for the rate of refinement of the internal structure to decrease after a long period of processing because the particles get exceedingly hard. The hardness is the result of the accumulation of strain energy. Eventually, a constant value called the saturation hardness is obtained. It was reported that true alloying has reached a significant point when the layers of a particle can no longer be optically resolved.

Based on powder particle size and impact energy required, balls with size of 10 to 30 mm are ordinary used. If the size of the balls is too small, impact energy may be too low for alloying to take place. In order to increase impact energy without increasing the rotational speed, balls with high density are employed.

Sometimes lubricants such as kerosene or fatty acids are added to prevent the particles from coming in contact. Although lubricants make finer grinding possible, they may severely contaminate the powders and degrade the alloy made from them.

2.5 Effect of Copper on FeSi$_2$

The mechanism of Cu to accelerate the reactions is liquid phase of Cu during annealing. Generally, liquid phase sintering is very effective for densification due to rearrangement of the particles [54]. There is the fact that Cu is not soluble in the β-

phase, but it is soluble in the α-phase and ε-phase [36]. When the β-phase decomposes to the α-phase and ε-phase at about 1253K, Cu in the liquid phase diffuses into the matrix of the α + ε phase and the amount of liquid phase decreases. During the reaction of α → β + Si, Cu in the α-phase is left because it has no solubility in the β-phase. This remaining Cu reacts with the Si phase and produces the Cu-Si liquid phase. In the sample with Cu, the reaction of α → β + (Cu+Si)$_{liquid}$ occurs instead of α → β + Si. The Cu-Si liquid phase helps to supply the α-phase as well as ε-phase with Si because the liquid phase spreads over the compact through inter-particles and the grain boundary [36].

CHAPTER III

EXPERIMENTAL METHOD

3.1 Sample Preparation Overview

Powders of Si (<78µm, 99%), Fe (<60µm, >99.0%) and Cu (3µm, 99.7%) elements were used as starting materials for this experiment. Nominal alloy compositions prepared in the present work are shown in Table 3-1.

Table 3-1: Nominal alloy composition (at.%)

Alloy	Fe	Si	Cu
$Fe_{30}Si_{70}$	30.0	70.0	0.0
$Fe_{29.9}Cu_{0.1}Si_{70}$	29.9	70.0	0.1
$Fe_{29.8}Cu_{0.2}Si_{70}$	29.8	70.0	0.2
$Fe_{29.5}Cu_{0.5}Si_{70}$	29.5	70.0	0.5

Mechanical alloying was carried out in FRITSCH pulverisette (Germany) planetary ball mills, with stainless 4 inches diameter milling bowl. Stainless steel balls of 10 mm diameter with 4.02g weight were used in this work. First of all, the suitable milling time must be determined. The powder of $Fe_{30}Si_{70}$ was milled under Ar atmosphere and examination by X-ray diffraction (XRD) and Scanning electron microscope (SEM) for various times. After MA processing, powder will be prepared for solidification process by sieving to -80 meshes. It could help to reduce crack on sample. The mixture will be split to solidify by 2 methods. First method, the 1.60 g milled mixture will be cold compacted into a bar shape 13.2 x 32.3 x 1.9 mm³ by applying the appropriate pressure. A set of these samples will be annealed in a furnace with a protective atmosphere of argon gas at 1073 K and 1173 K for various annealing time for 1, 3 and 5 hours.

Another method, the milled mixture will be hot-press into disc of 50-mm diameter depend on die and 1 mm thick which applied appropriate pressure at 1173 K for 1 hour soaking time.

Finally, Seebeck coefficient of all samples was measured by self-constructing equipment. This equipment was verified by measured Seebeck coefficient of Cu at room temperature.

3.2 Milling Process

To prevent contamination from milling bowl and balls, Si and Fe powder were pre-milled in order to enamel the bowl and the balls before milling per the composition. Silicon will coat milling pot and stainless balls.

Both continuous milling and stepping milling were tried. Continuous milling could create sticking problem of mixture to the milling bowl and balls. Improper milling step also cause as the sticking problem as well. During trial in milling process, there are some observations as followings. Firstly, decreasing milling speed could help to reduce the sticking problem. Normally, the milling impact frequency will decrease when milling speed decrease. However, low milling speed is not the key solution to eliminate the sticking problem. Mixture was milled with interval breaks.

Next, we also tried to add hexane to act as a lubricant and heat transfer liquid in order to prevent the sticking problem. The advantage of hexane addition is creating homogeneous reaction. In contrast, the activation energy will be decreased from hexane. It will act as coolant and decelerator of ball speed. However, we expect that hexane might save preparation time. Due to design of milling pot, the mixture milling with hexane was performed under normal atmosphere.

3.3 Cold Pressed Process

Solidification techniques by cold press method were tried. Pressing force was 15 tons with 2 minutes clamping time. During trial and error for several times, it was found that there is a vibration of the equipment when mold press cavity move down to press and/or up to de-press the mixture. Thus, speed of mold press cavity movement should be set at the slowest to let mold press cavity move smoothly. This can reduce vibration of the system to prevent crack problem on sample. In addition, the mixture was sieved before pressing process. This can also prevent the mixture hold together and therefore has internal void during pressing process. It is another potential cause of the crack problem. Furthermore, method of sample keeping from the cavity is important too. To gentle keep the sample from the cavity could reduce defect rate of pressing process. Finally, well spreading the mixture whole the cavity could also help the mixture completely form into non-defect piece.

3.4 Annealing Process

We annealed each composition of mixture at 2 different temperatures, 800°C and 900°C. All samples were annealed under Ar atmosphere. Annealing time is the one important parameter. Three different soaking annealing times for each temperature were defined at 1, 3 and 5 hours. Therefore, total prepared samples are 24 samples. In the other word, we must use each mixture for 6 pieces.

Temperature-time relation is shown in Figure 3-1. In the first annealing period, the temperature was raised up with 10ºC per minute until reach the set point temperature. In the middle annealing period, temperature in furnace was kept at set point temperature until complete setting soaking time. And in final annealing period, temperature in furnace was cold down with the same rate as ramp up rate until reach about 200°C to prevent heater damage, then, free convection.
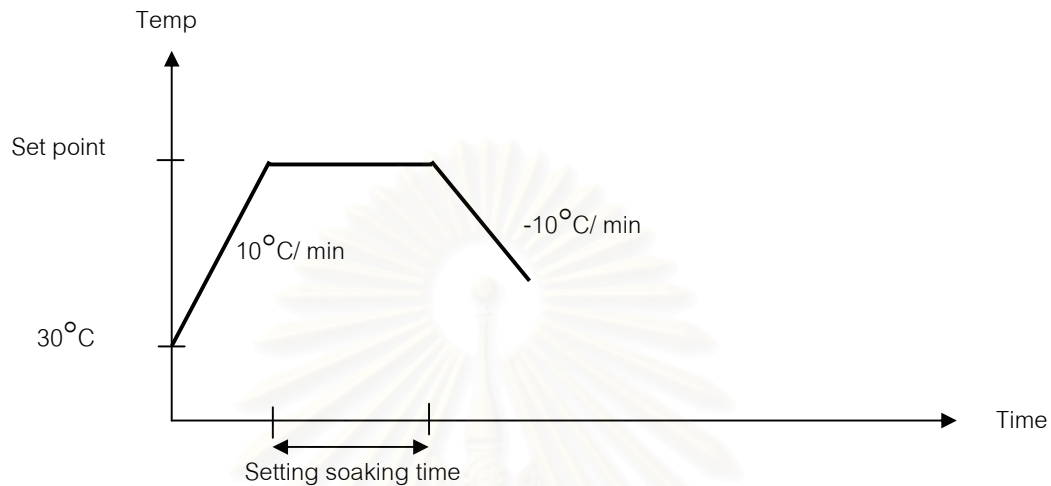
Figure 3-1: Temperature profile of annealing process.

After annealing, all samples were performed XRD and Seebeck coefficient measurement. The results were in chapter IV.

3.5 Hot Pressed Method

We have prepared some samples by using hot-press method. All hot pressed samples were prepared under Ar atmosphere. Boron Nitride sprays layer on Die and Mold was used in order to prevent element from Die and Mold react with sample during apply pressure and temperature. The condition of hot pressing which is shown below was applied to all samples preparation.

In ramp up period, starting with room temperature, furnace temperature was ramped up with 10C°/ min ramp up rate until reach 900°C with 5 Mpa pressure. When furnace temperature reached 900°C, temperature was kept at 900°C for 1 hour with 26 MPa pressure. After complete 1 hour of soaking time, this pressure was maintained until furnace temperature cold down to room temperature. The temperature was cold down

with the same rate as ramp up rate until reach about 200°C to prevent heater damage, then free convection. Temperature and pressure profile were illustrated as profile in Figure 3-2.
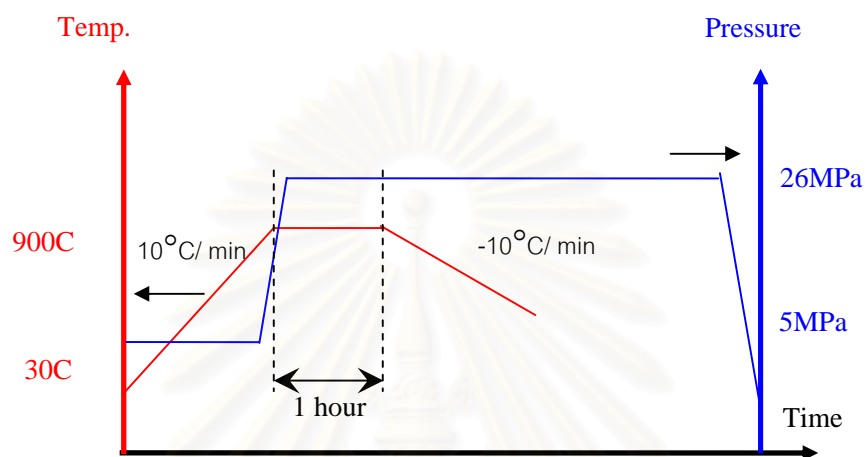

Figure 3-2: Temperature and pressure profile of hot press process.

After hot pressing, all samples were performed XRD and Seebeck coefficient measurement. The results were in chapter IV.

3.6 X-ray Diffraction

In order to investigate the degree of alloying and phase transformation during milling and sintering, X-ray diffraction (XRD) analysis was carried out for the mixture and annealed samples. A Philips ($X^{'}$pert) x-ray diffractometer system with Cu-Kα radiation (λ = 1.54060 A°) was used at 40 KV with current 30 mA. We used PDF (Powder Diffraction File) database as the reference for phase determination as shown in following figures.
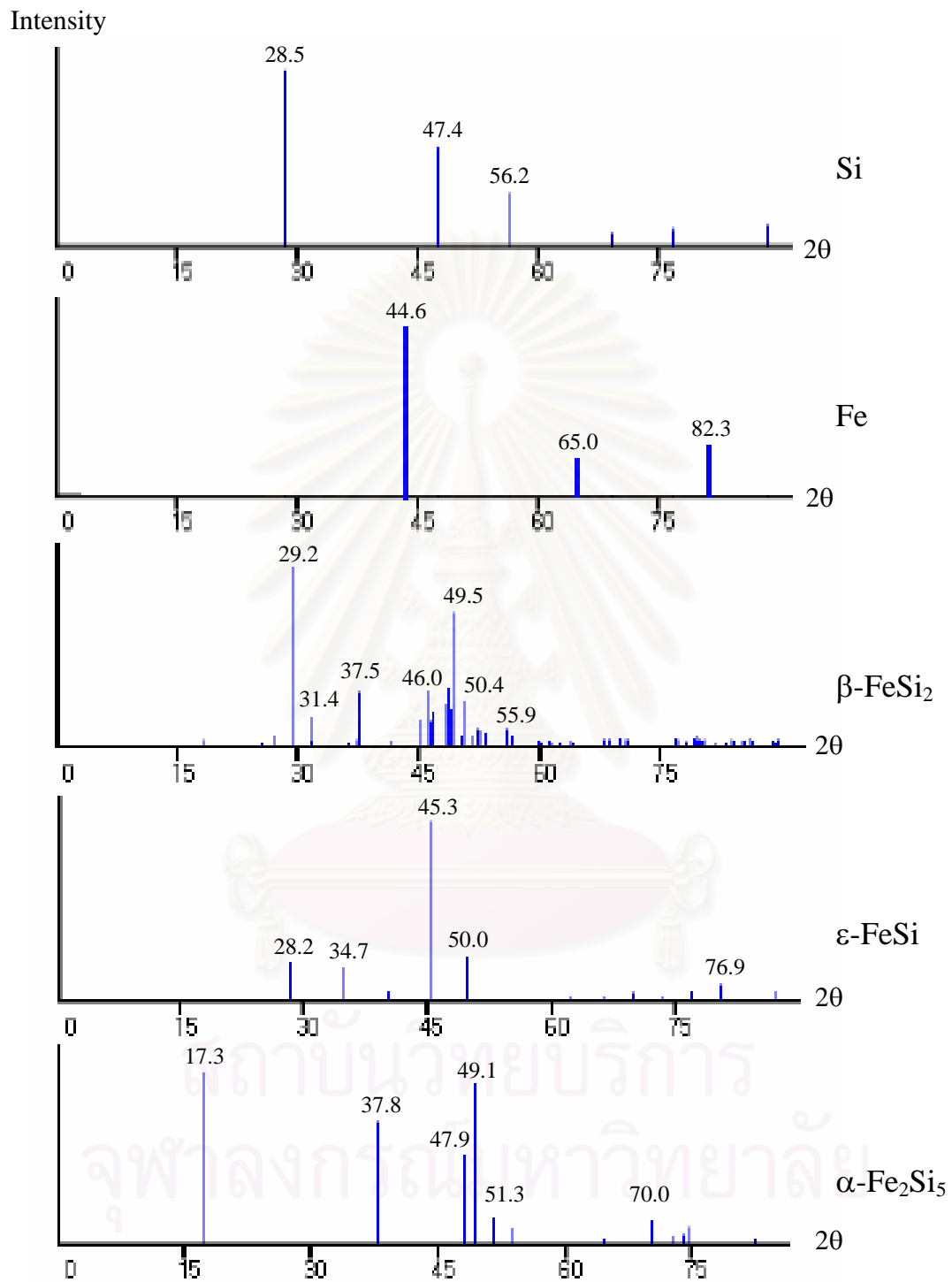
Figure 3-3: XRD peak patterns of silicon, iron, β-FeSi$_2$, ε-FeSi and α-Fe$_2$Si$_5$.

3.7 Scanning Electron Microscopy

Grain size of mixture at each total milling time was determined by a Jeol (JSM 5410LV) scanning electron microscopy (SEM). We prepared sample by cutting it into specimens with dimensions suitable with stubs. Importantly tall samples can damage the objective lens pole piece if moved to high. Samples were stuck with stubs by electrically-conductive carbon tape. All mixtures were coated gold to make them conductive.

3.8 Seebeck Coefficient Measurement

Seebeck coefficient was determined by the ratio of an open-circuit potential difference to a temperature difference. The temperature difference is measured by using chromel-alumel (K-type) thermocouples, and the copper branches are also used to obtain the potential difference which is shown in Figure 3-8. The reference junctions of the thermocouples fixed with a heat sink whose temperature is close to the room temperature. The potential differences between V_1 and V_2 will be read by a Keithley digital multimeter model 2700. The probe is connected to a thermocouple measureing the temperature T_1 at the probe tip. The sample contact to a heat sink whose temperature T_0 is measured by another thermocouple. The copper was used to measure the potential difference, ΔV, across the sample.
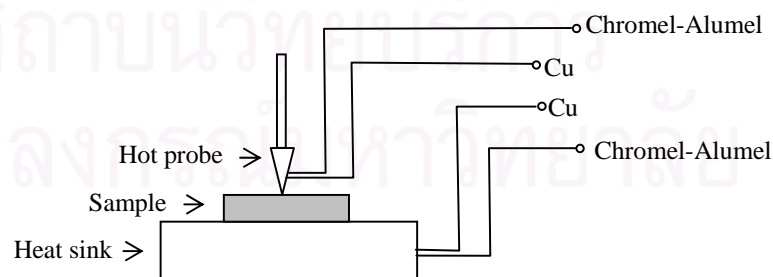

Figure 3-4: Illustration of Seebeck coefficient measurement equipment.

CHAPTER IV

RESULTS AND DISCUSSIONS

4.1 Preparation

4.1.1 Milling process

All mixtures were milled with milling speed 295 rpm. Ball to powder weight ratio was fixed at 10:1. The longest milling time which we used was 110 hours. However, XRD and SEM results of mixture milling for 110 hours did not show significantly different from that of 50 hours. See Figure 4-1 for XRD results of Cu free mixtures. The XRD results of Cu free mixtures milling for 50, 70 and 110 hours show no peaks of Si and Fe. Only α, ε and β phases could be observed. And XRD results of the mixtures milling for 70 and 110 hours show no significantly different from that of the mixture milling for 50 hours. Figure 4-2 is XRD result of 0.1%Cu added mixtures. The XRD results of Cu free mixtures milling for 50, 70 and 110 hours show no peak of Si, Fe and Cu. Only α, ε and β phases could be observed. And XRD result of the mixtures milling for 70 and 110 hours also show no significantly different from that of the mixture milling for 50 hours like the results of Cu free mixtures. In addition, the XRD results of the Cu added mixtures are no significantly different from Cu free mixtures at each milling time. The added copper did not effect on phase formation in milling process.
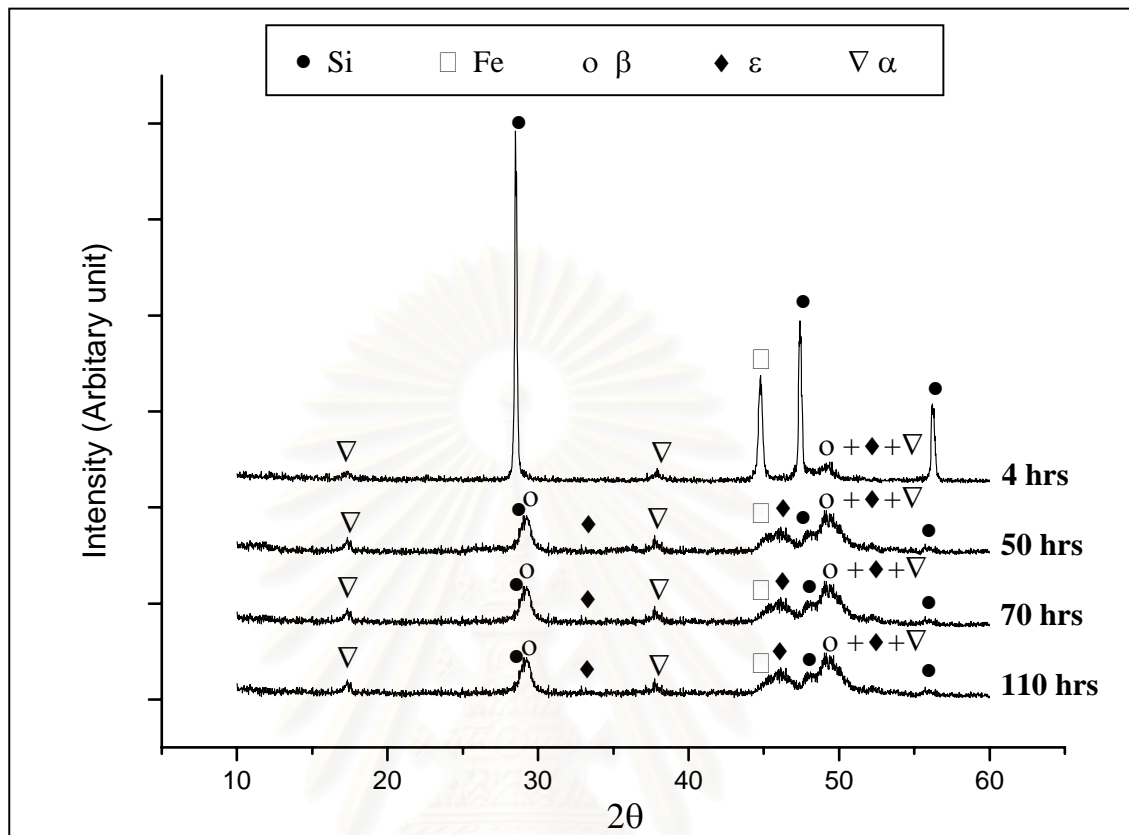
Figure 4-1: XRD results of Cu free mixtures after milling for 4, 50, 70 and 110 hours.
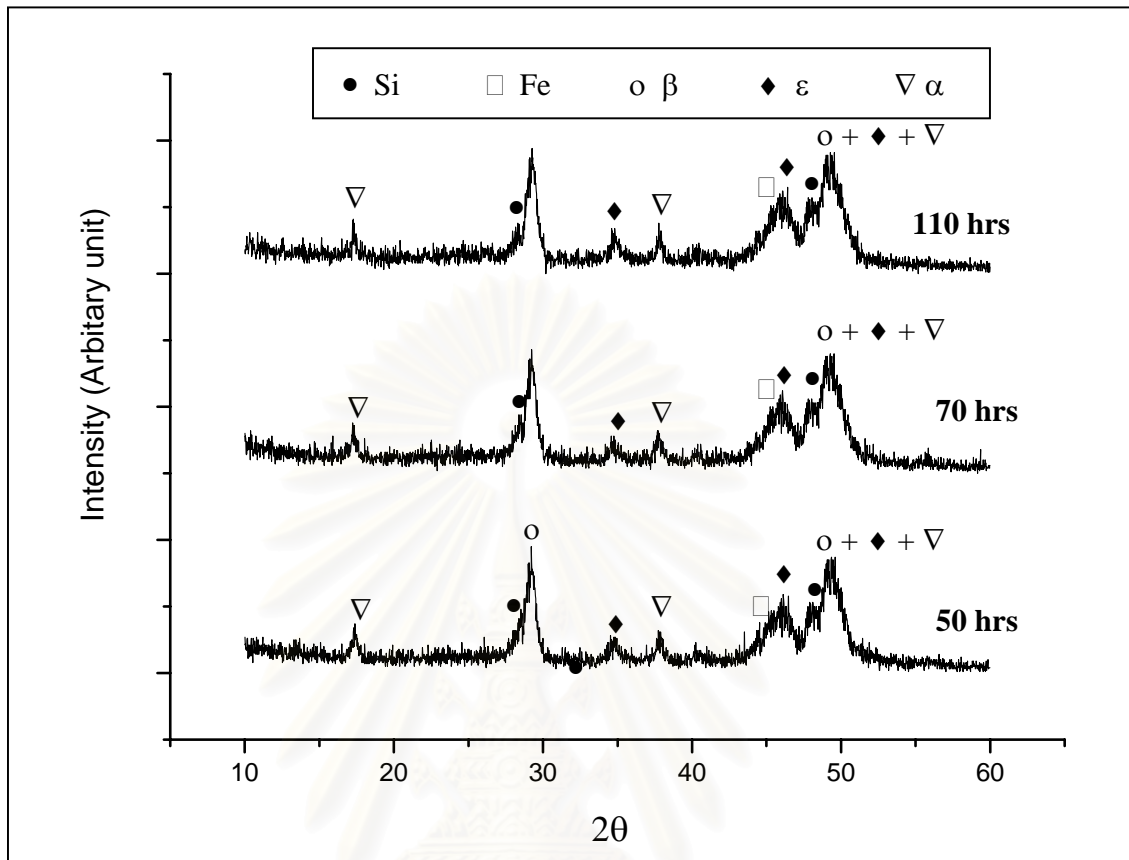
Figure 4-2: XRD results of 0.1% Cu added mixtures after milling for 50, 70 and 110 hours.

SEM results show that the particle size of mixture milling for 32 hours did not significantly different from that of mixture milling for 72 hours. See Figure 4-3 for SEM results. The mixtures after milling for 4 hours, 8 hours, 32 hours and 72 hours show average particle size of 5- 10 µm, 1-5 µm, 0.5-2 µm and 0.5-1 µm, respectively. From XRD and SEM result, we selected 50 hours total milling time for this work because there is no significantly change of mixture after milling longer than 50 hours. This total milling time agrees with publication of Min et al [30] who had milling for 50 hours. And their SEM result show particle size approximately 1.2 µm which is in line with our work.
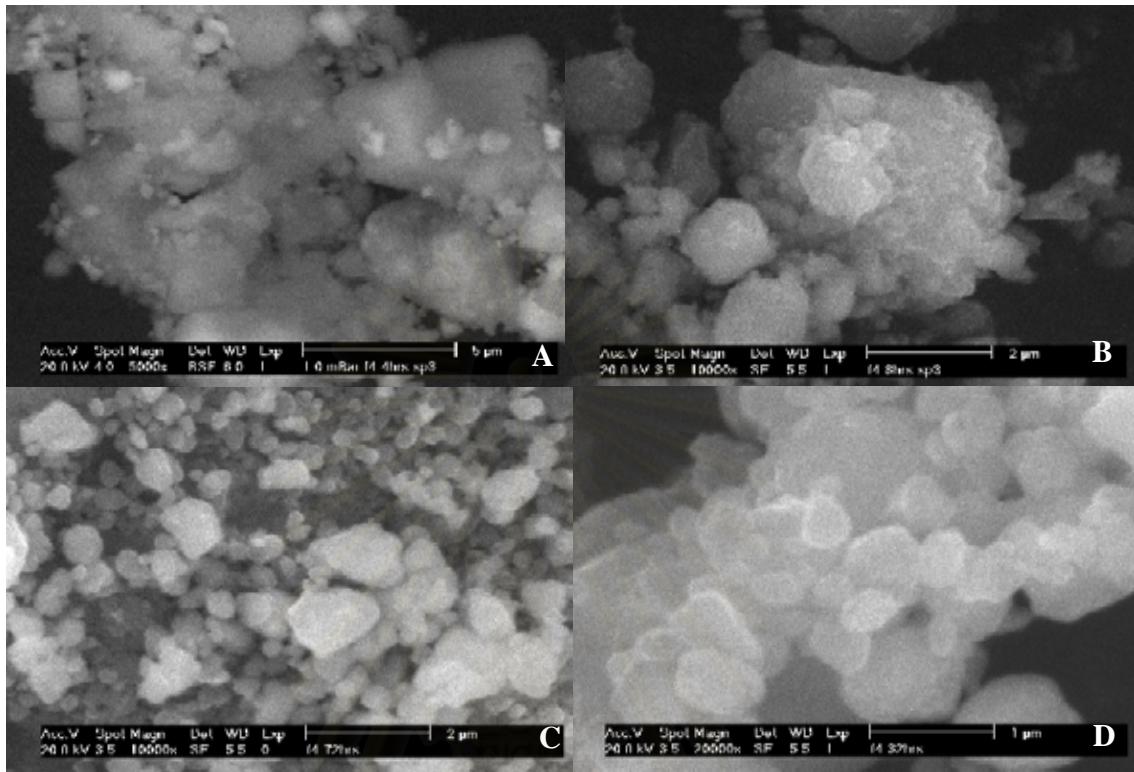
Figure 4-3: SEM results of (A) mixture after milling for 4 hours show average particle size 5 – 10 µm, (B) mixture after milling for 8 hours show average particle size 1 – 5 µm, (C) mixture after milling for 32 hours show average particle size 0.5 – 2 µm and (D) mixture after milling for 72 hours show average particle size 0.5 – 1 µm.

There is no paper which describes the milling recipe. Some works reveal that lubricant was added during milling process. However, the added lubricant did not be specified. Rowe [4] guides milling process should have pattern. We noted that heavily milling in initial phase of milling with scratch the mixture during milling break play the important rule of prevent the sticking problem. This may be because Si and Fe powder have been mixed adequately. After several times of trial with analysis, we got the appropriated milling pattern which is divided into two phases as charts in Figure 4-4 and Figure 4-5:
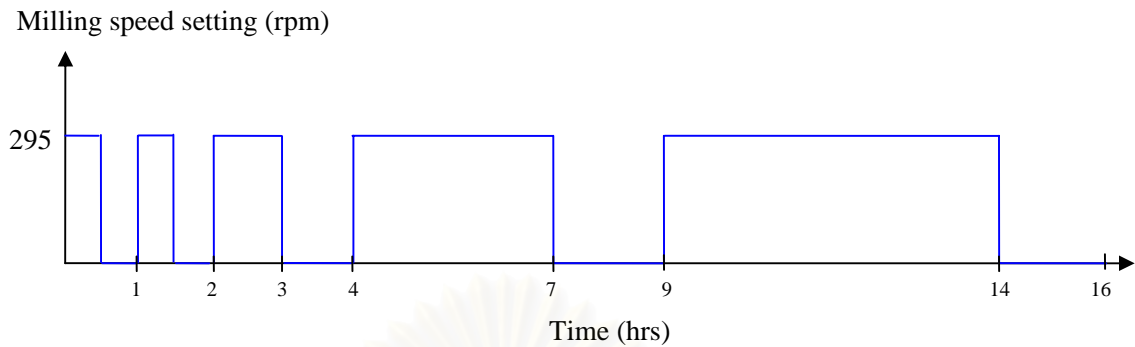
Milling speed setting (rpm)

Figure 4-4: Profile of initial phase of milling process.
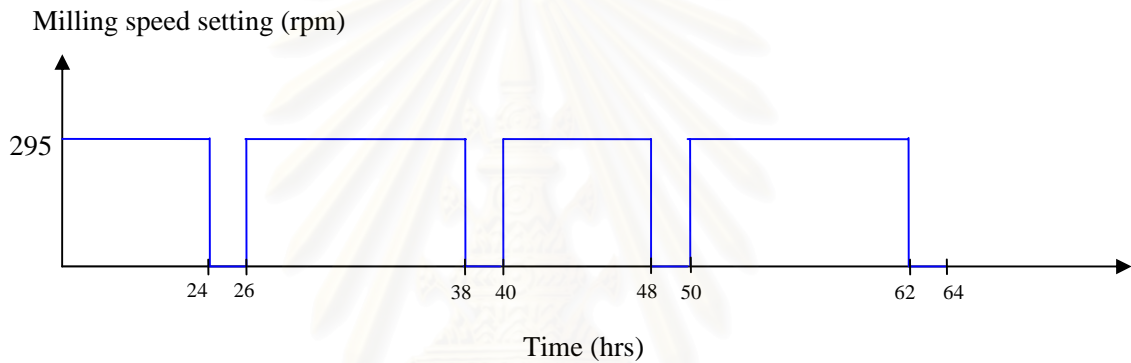
Milling speed setting (rpm)

Figure 4-5: Profile of final phase of milling process.

In this work, we get milling recipe to get the mixture without sticking problem which starting with <78μm for Si and <60μm for Fe. 50 hours total milling time from total spending 64 hours with milling speed 295 rpm. 78.1% utilization, which is the ratio of machine working time to total time, of milling process could be calculated. From our milling recipe, it could be divided into 2 milling phases. The first phase is in first 10 hours total milling time. 62.5% utilization of the first phase of milling process could be calculated. Compare with the second phase which is in last 40 hours total milling time, it was 83.3% utilization. One can see that quite low utilization of milling process in the first milling phase can be the cause of low overall milling utilization. The reason why the first milling phase has quite low milling utilization is to prevent sticking problem of the mixture. There is severe sticking problem in period of the first milling phase. Because Fe and Si still not are mixed enough, stickiness of Fe could hold each other and could hold the wall.

4.1.2 Milling Process with Lubricant

After finishing 50, 70 110 hours milling time, there is tough liquid to wet around joint between milling bowl and its lid. It was supposed to be solution between hexane and seal material. In addition, we had to refill hexane during stopping time because some hexane was evaporated from high temperature. Gushing of hexane when the lid was opened is the one of evidence. The dry mixtures of each milling time were performed XRD measurement. XRD results were shown in Figure 4-6. XRD results of mixture milling for 110 hours did not show significantly difference with the results of mixture milling for 50 hours. The XRD results of mixture after milling for 50, 70 and 110 hours show no peak of Si and Fe. α, ε and β phases could be observed. And there is another unidentified peak of 2θ at $40°$ as a sign of contamination.
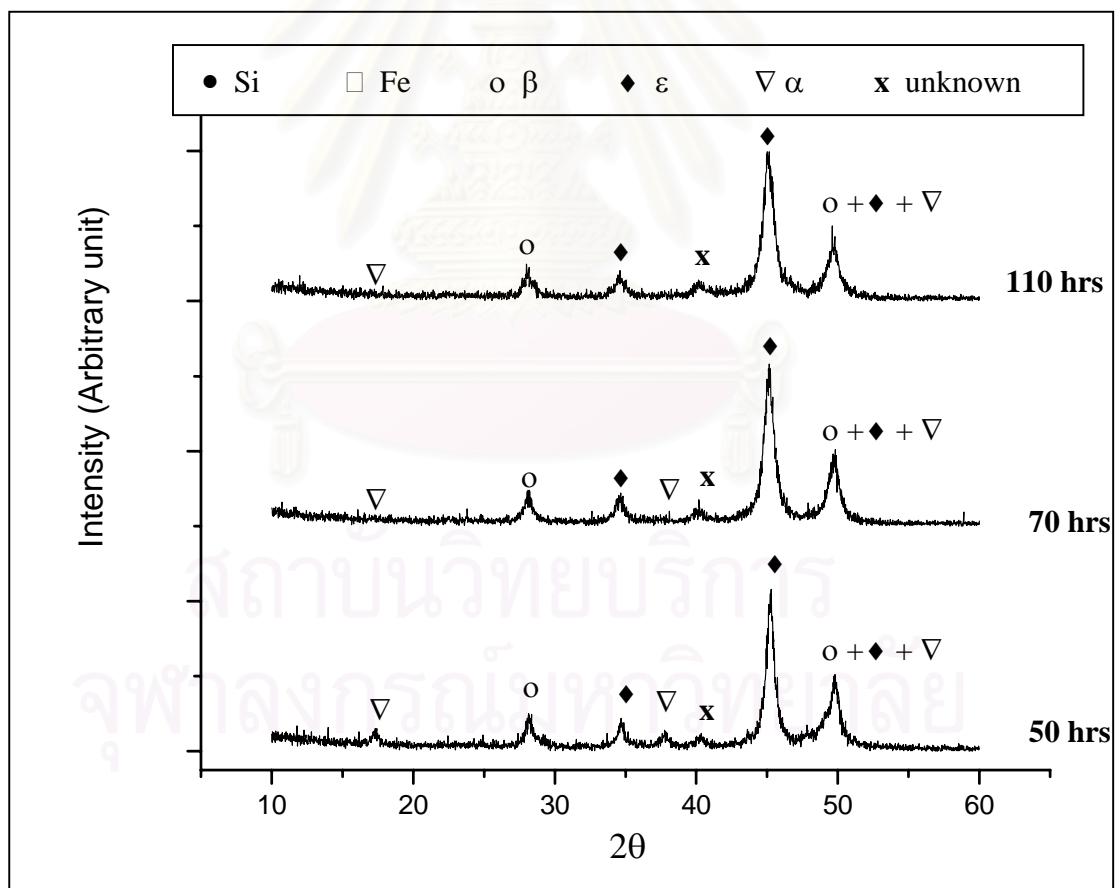

Figure 4-6: XRD results of mixtures after milling with hexane for 50, 70 and 110 hours.

The XRD results indicated that milling the mixture with hexane should be studied and improved in future work. There are several reasons to support the result. First of all, this milling condition was milled under atmosphere due to limitation of the equipment. Moreover, seal material might contaminated in the substance once hexane is the dissolution. Contamination problem could be confirmed by XRD result. In addition, hexane may be left behind in the substance after it was dry. With lubricant of hexane, unsafety condition occurs during preparation. There is vapor pressure of the lubricant (Hexane) due to kinetic energy of milling ball and therefore thermal energy. Due to severe contamination problem, hexane is forbidden to add in the mixture to play the role of lubricant. However, for future work, there are some publications which reveal kind of the lubricant consisting of 0.8wt% polyvinyl alcohol and ethyl alcohol [28]. In conclusion, we should improve the milling method because the mixture quality can be controlled.

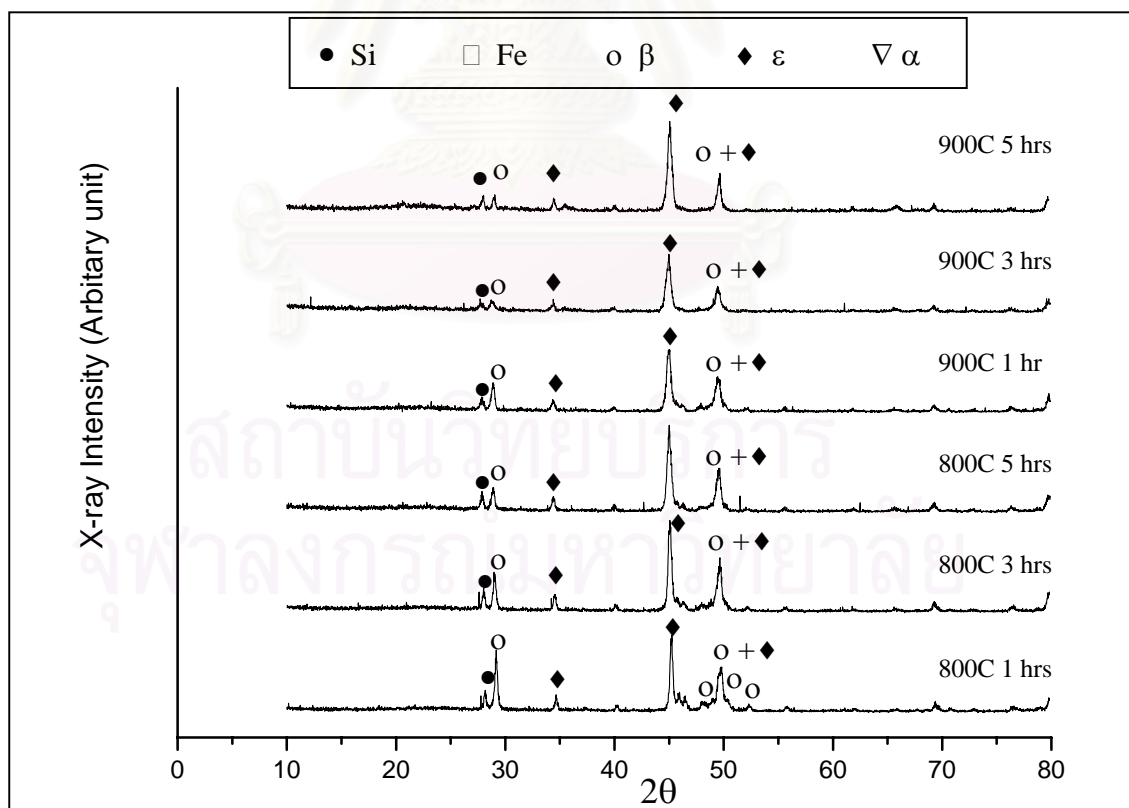## 4.2 XRD and Seebeck Result of Cold Pressed Samples

Figure 4-7: The XRD result of Cu-free FeSi$_2$ samples for each preparation condition.
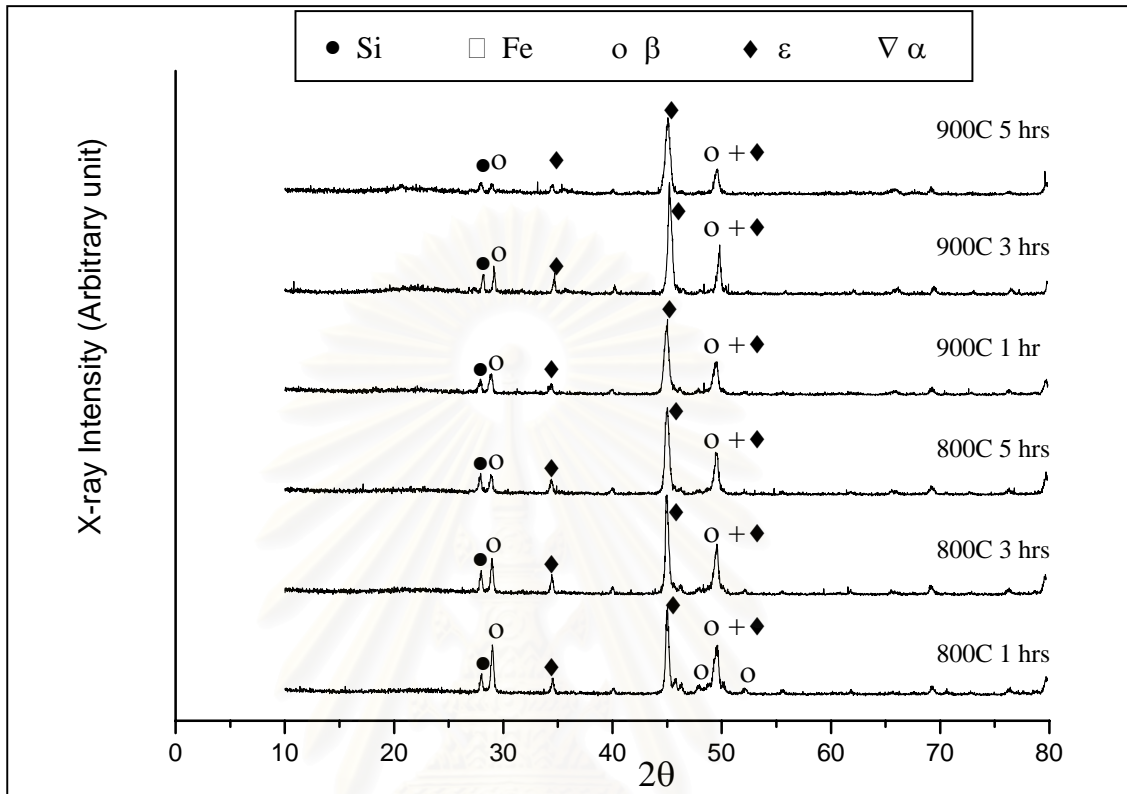
Figure 4-8: The XRD result of 0.1%Cu added $FeSi_2$ samples for each preparation condition.

All cold pressed samples were preformed XRD in order to examine β phase of each preparation condition. The XRD results of Cu free samples and 0.1%Cu added samples were shown in Figure 4-7 and Figure 4-8, respectively. For 0.2%Cu added samples and 0.5%Cu added samples showed similar result like that of 0.1%Cu added samples and Cu free samples. All cold pressed samples showed majority of ε-FeSi phase. Si and β-$FeSi_2$ phase could be observed from XRD result while α-Fe_2Si_5 disappeared. Fractions of Si, β-$FeSi_2$ and ε-FeSi were calculated to indicate the amounts of each phase of each samples. Phase fractions of Si, β and ε were calculated from the intensity of the principal peak at 2θ of 28.5, 29.2 and 45.3, respectively as following:

$$\text{fraction of Si} \; = \; \frac{I_{Si}}{I_{Si} + I_{\beta} + I_{\varepsilon}} \, , \qquad\qquad (6)$$

$$\text{fraction of } \beta \; = \; \frac{I_{\beta}}{I_{Si} + I_{\beta} + I_{\varepsilon}} \, , \qquad\qquad (7)$$

$$\text{fraction of } \varepsilon \; = \; \frac{I_{\varepsilon}}{I_{Si} + I_{\beta} + I_{\varepsilon}} \, , \qquad\qquad (8)$$

The fractions were plotted for comparison with Seebeck coefficient result in Figure 4-9 and Figure 4-10 where annealing time was varied and in Figure 4-13 where Cu content was varied.
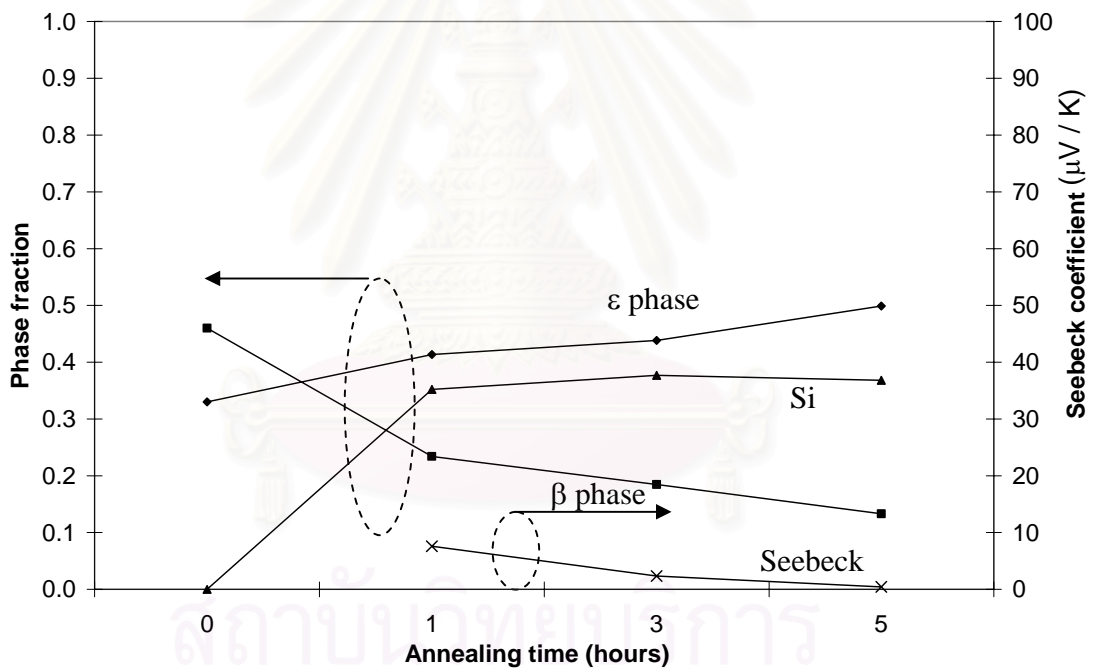
Figure 4-9: Phase fraction and Seebeck coefficient of Cu free cold pressed sample annealing at 800°C by varies annealing time.
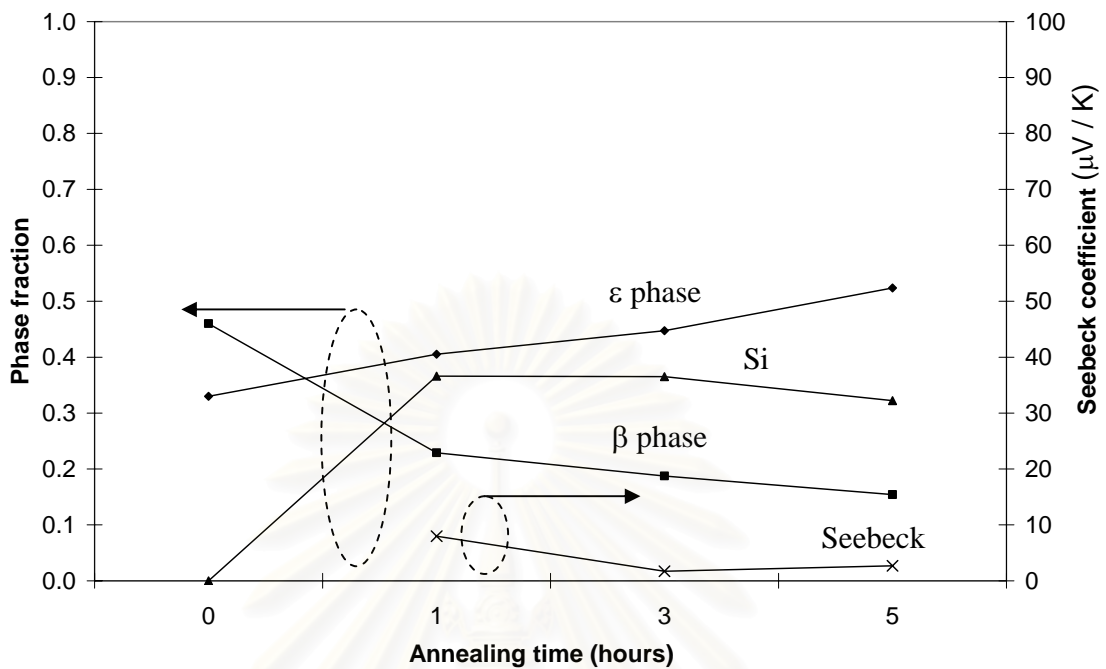
Figure 4-10: Phase fraction and Seebeck coefficient of 0.1%Cu added cold pressed sample annealing at 800°C by varies annealing time.

Seebeck coefficient of all cold pressed samples was measured. Each Seebeck voltage was recorded for each average measured temperature of the system as shown in Table 4-1. For cold pressed samples, it was found that the signs of their Seebeck coefficient are positive. Their voltage potential of the cold side with respect to the hot side is positive. It means all cold pressed samples are P-type semiconductor.

Table 4-1: Seebeck coefficient of cold pressed samples.

Composition	Anneal condition	Seebeck coefficient for different temperature range (μV / K)				
		300 - 305K	305 - 310K	310 - 315K	315 - 320K	320 - 325K
Cu free	800C 1hr	7.096	7.227	7.487	7.586	7.640
	800C 3hrs	1.193	1.575	2.030	2.335	2.783
	800C 5hrs	noise	0.109	0.200	0.438	0.650
	900C 1hr	6.487	7.158	7.802	8.292	8.872
	900C 3hrs	4.117	4.570	4.786	5.211	5.596
	900C 5hrs	1.507	1.803	2.157	2.507	2.797
0.1%Cu	800C 1hr	4.276	6.015	7.176	7.985	8.931
	800C 3hrs	0.877	1.252	1.569	1.702	1.841
	800C 5hrs	1.767	1.839	2.202	2.686	3.013
	900C 1hr	6.311	7.206	8.129	8.344	12.002
	900C 3hrs	3.700	3.720	3.732	3.745	3.769
	900C 5hrs	2.105	2.599	3.164	3.827	4.447
0.2%Cu	800C 1hr	5.217	6.058	6.865	7.696	8.467
	800C 3hrs	2.795	2.986	3.083	3.639	4.590
	800C 5hrs	1.552	1.580	1.632	2.004	2.597
	900C 1hr	3.818	4.246	4.727	5.321	5.914
	900C 3hrs	3.473	4.390	5.134	5.936	6.695
	900C 5hrs	0.411	0.512	0.682	1.041	1.383
0.5%Cu	800C 1hr	7.298	8.066	9.047	10.077	11.099
	800C 3hrs	2.534	3.185	3.731	4.349	4.687
	800C 5hrs	1.648	1.889	2.335	2.806	3.212
	900C 1hr	11.362	12.566	13.864	15.125	15.998
	900C 3hrs	6.655	7.101	7.480	7.835	8.079
	900C 5hrs	1.838	2.079	2.346	2.616	2.782

0.2%Cu added samples and 0.5%Cu added samples showed similar result like that of 0.1%Cu added samples and Cu free samples. β phase tends to decrease with increasing annealing time while ϵ phase and Si tend to increase. Seebeck coefficient also tends to decrease with increasing annealing time. Increasing of metallic ϵ phase with decreasing of semiconducting β phase is known to result in the decreasing of Seebeck coefficient of the samples.

We believed that the amount of β-FeSi$_2$ diminished with increasing annealing time because of the un-stability of β-FeSi$_2$ phase. And decreasing trend of Seebeck coefficient and β phase fraction should be from the remained large size of Fe particles. From Master's thesis of Jamreonta Parinyataramas [55], who used the same starting material, the same milling equipment and the same milling pattern, the result of particle size distribution of the mixture milling for 50 hours show the remained of large Fe particle. See in Figure 4-11. The result of mixture milling for 50 hours has 2 groups of particle size consisting of 1 µm and 60 µm. The first group of particle of 1 µm should be Si because Si is hard and brittle. The second group of particle of 60 µm should be Fe because Fe is soft and ductile.
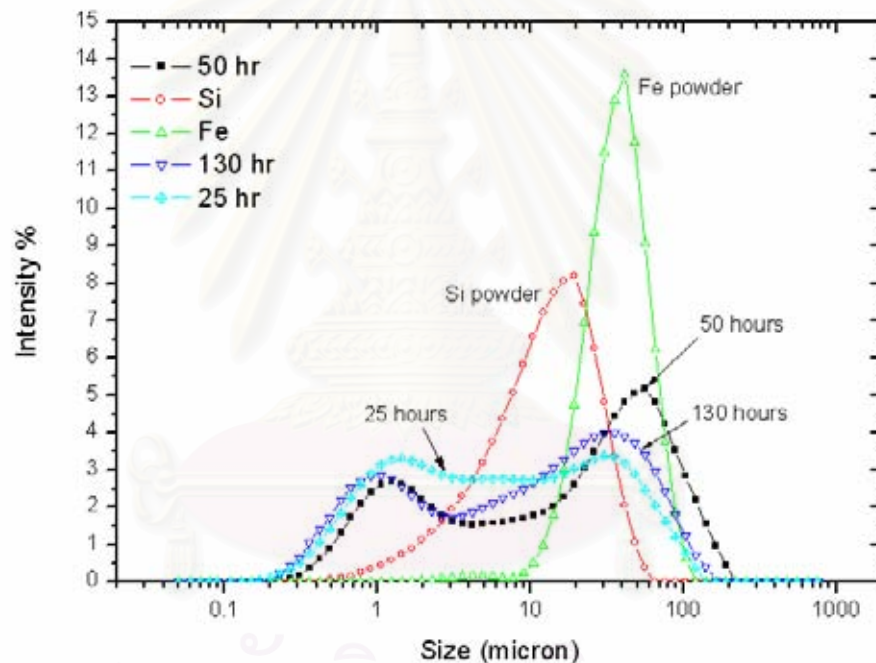

Figure 4-11: Particle size distribution of starting material and mixture after milling for 25 hours, 50 hours and 130 hours [55].

For the large particle we expect that the percent of composition in mixture between Fe and Si should not be 30 and 70, respectively. In contrast, %Fe could be higher than %Si. From empirical phase diagram as in Figure 4-12, at the annealing temperature, the phase in which the mixture should develop is metallic ε-phase. So, the longer annealing time, the less semiconducting Si phase with the more metallic ε-FeSi phase. This could be the cause of reducing Seebeck coefficient as well as β phase.

However, very long annealing time until the whole sample reach to equilibrium phase, where balancing between Fe and Si occur, β phase could be grown. And the degree of homogeneity attained in the final product is limited by the size of particles in the powders. If the particles are too coarse, the different ingredients will not easily inter-diffuse during heat treatment.
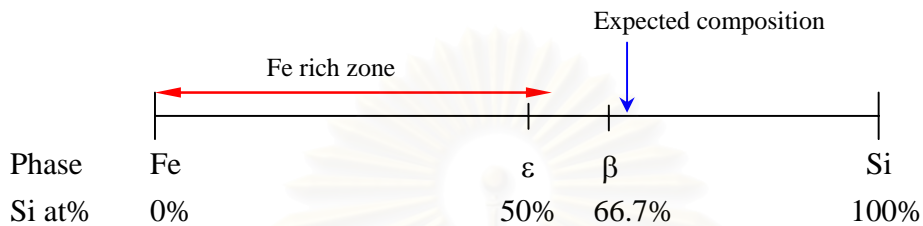

Figure 4-12: The empirical phase diagram of Fe-Si system.

For phase fraction and Seebeck coefficient of cold pressed samples with various Cu content is plotted in Figure 4-13. β phase and ε phase tend to slightly increase with increasing of Cu content while Si tend to decrease. However, increasing of ε phase with Cu content is faster than that of β phase. Increasing of semiconducting β phase results in the increasing of Seebeck coefficient of the samples.
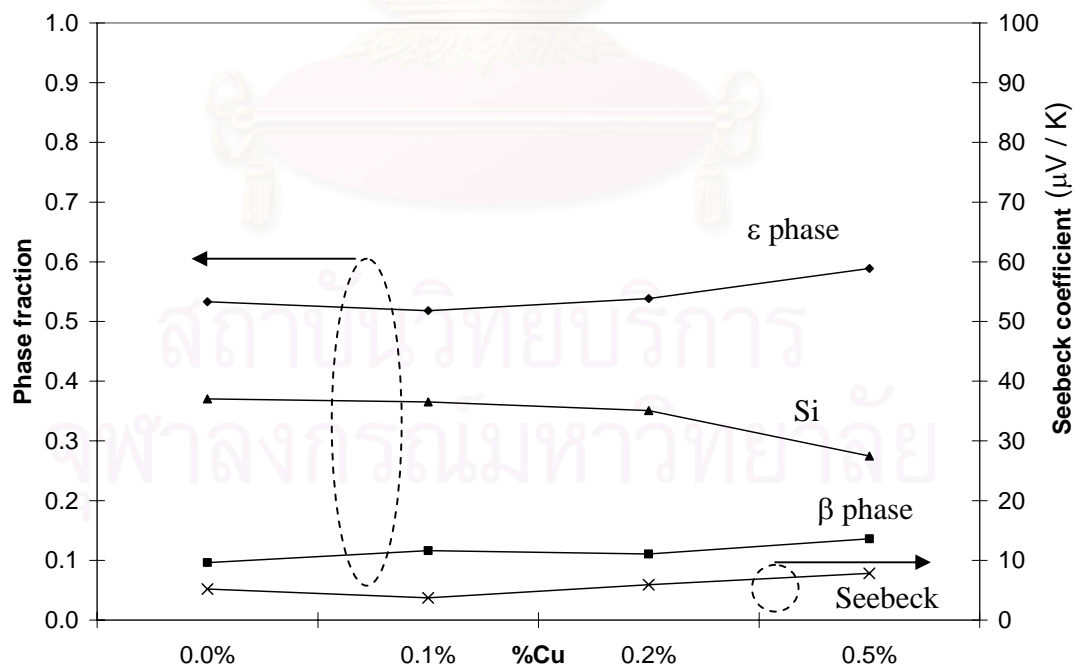

Figure 4-13: Phase fraction and Seebeck coefficient of cold pressed samples annealing at 900°C for 3 hours by varies %Cu addition.

Therefore, 1 hour annealing time with 0.5%Cu added cold pressed sample give the highest β phase and Seebeck coefficient of 16 µV/K at room temperature. The effect of Cu addition into $FeSi_2$ was reported to accelerate the kinetics of ε to β conversion upon heat treatment [23, 56, 57] as well as the decomposition [40, 56]. Kinetics for this conversion has been known to be sluggish [22], because the peritectoid reaction (α + ε → β) is controlled by the diffusion through the newly formed solid β [23, 56, 58, 59]. The Cu addition could increase diffusion rate of Si particle due to liquid phase of Fe-Si system above 800°C during annealing process [23, 39, 40]. Thus, the result of increase Cu content is to increase β phase in sample. However, unstability of $β-FeSi_2$ phase was believed to be the cause of amount of $β-FeSi_2$ diminish with increasing of annealing time.

4.3 XRD and Seebeck Result of Hot Pressed Samples

All hot pressed samples were performed XRD in order to examine β phase of each composition as shown in Figure 4-14. All compositions show majority of $β-FeSi_2$ phase. ε-FeSi phase and silicon could be observed from XRD result while $αFe_2Si_5$ phase disappeared. Fractions of Si, $β-FeSi_2$ and ε-FeSi were calculated to indicate the amounts of each phase of each samples. The fractions were plotted for comparison with Seebeck coefficient result in Figure 4-15.

Seebeck coefficients of all hot pressed samples were measured. Each Seebeck voltage also was recorded for each average measured temperature of system as shown in Table 4-2. Like the result of cold pressed samples, the voltage potential of the cold side with respect to the hot side is positive. Therefore, the signs of their Seebeck coefficient are positive. It means all hot pressed samples are P-type semiconductor. Seebeck coefficient showed that 0.1%Cu added hot pressed sample gives the highest Seebeck coefficient of 66 µV/K at room temperature.
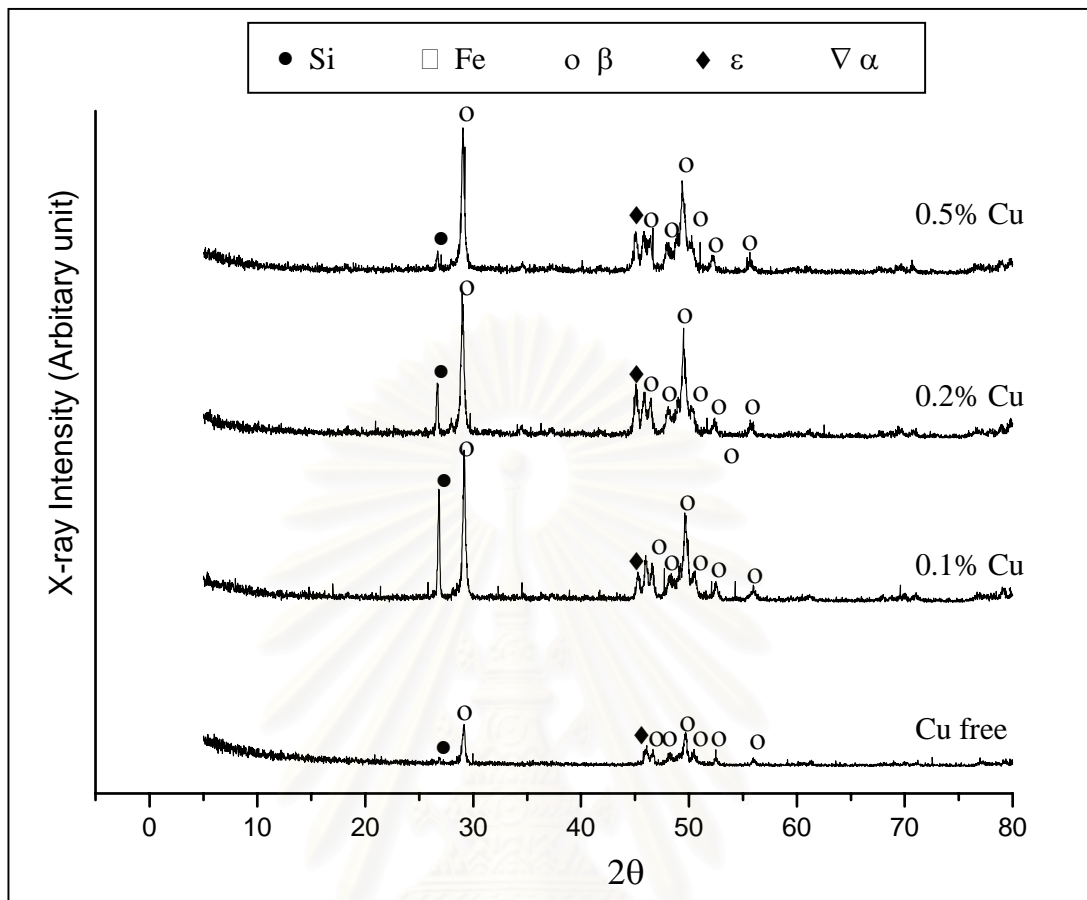
Figure 4-14: The XRD result of hot press FeSi$_2$ samples for each condition.

Table 4-2: Seebeck coefficient of hot pressed samples.

Composition	Seebeck coefficient for different measured temperature (µV / K)					
	296-300K	**301-305K**	**306-310K**	**311-315K**	**316-320K**	**320-325K**
Cu free	28.14	29.40	30.15	30.77	31.46	32.15
0.1%Cu	52.14	54.96	57.74	60.79	63.21	65.96
0.2%Cu	40.55	42.89	44.81	46.39	48.44	49.11
0.5%Cu	38.32	40.72	42.71	44.44	46.22	48.04

Figure 4-15: The plot between Seebeck coefficients against %Cu addition of hot pressed samples at 315K - 320K measured temperature.
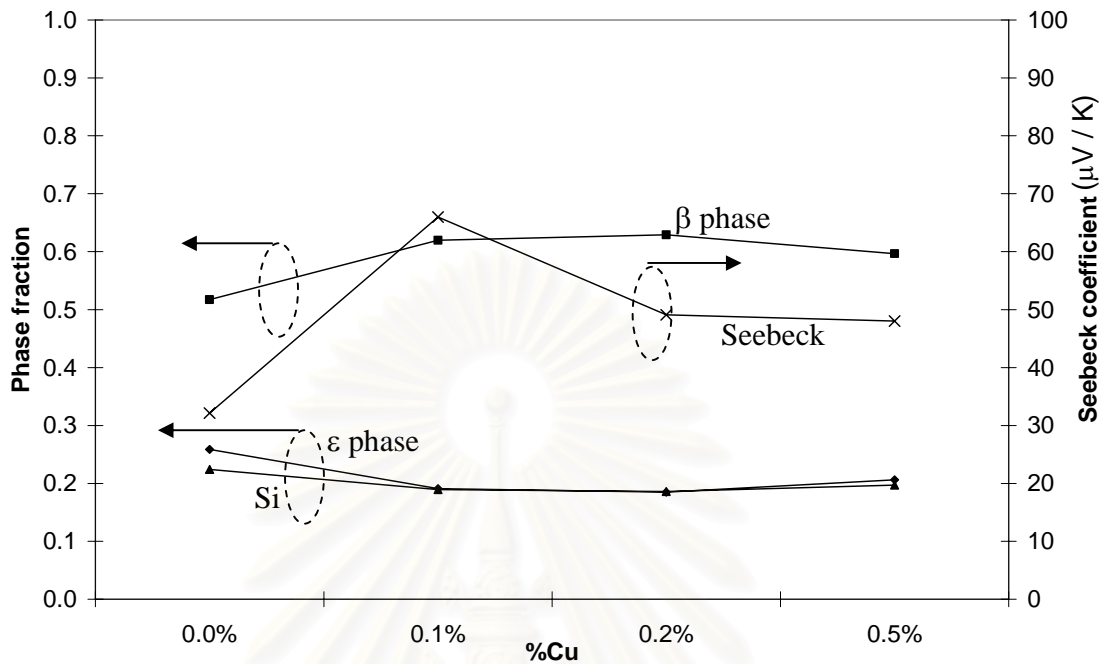
For hot pressed samples, β phase fraction and Seebeck coefficient is maximize with content of Cu around 0.1% - 0.2% while ε phase and Si are minimum. Increasing of semiconducting β phase with decreasing of metallic ε phase result in an increasing of Seebeck coefficient of the samples. This increasing of β phase fraction with increasing of Cu content is because addition could increase diffusion rate of Si particle as discussed in the result of cold pressed samples.

4.4 Cold Press Method and Hot Press Method Comparison

β phase fraction and Seebeck coefficient of both cold press and hot press method were plotted in Figure 4-16 for comparison.
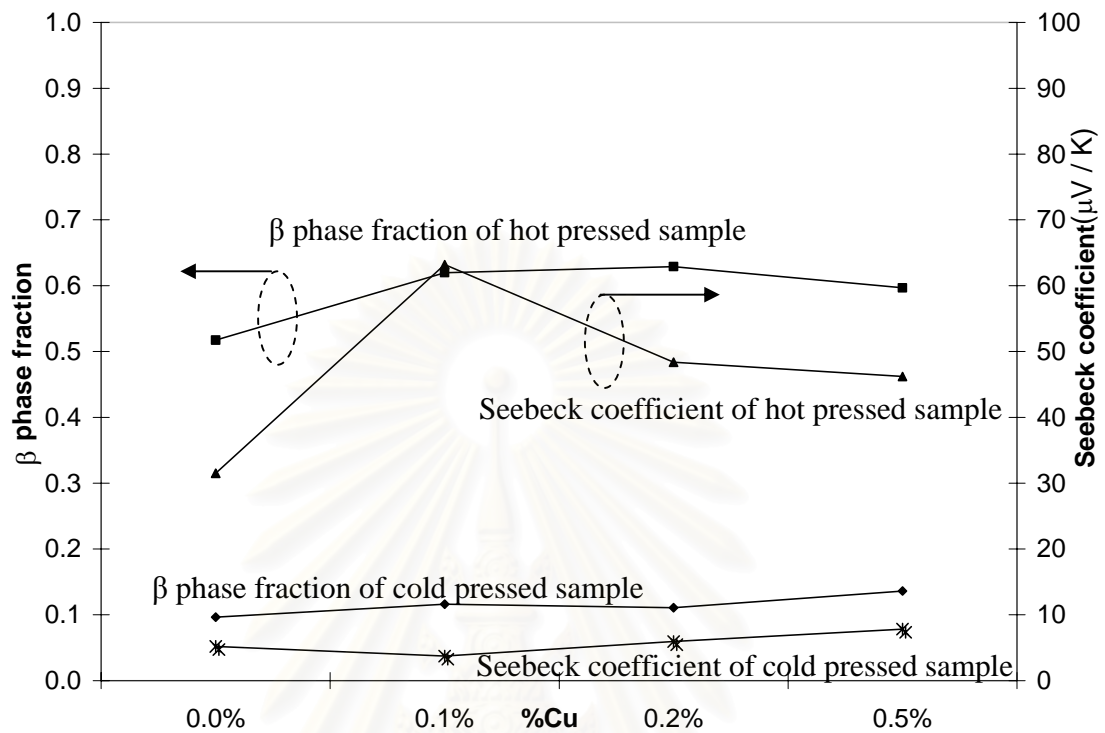
Figure 4-16: Chart of summary result of both XRD and Seebeck coefficient.

From Figure 4-16, β phase fraction and Seebeck coefficient of hot pressed samples were greater than those of cold pressed samples. This should be because the hot press method has higher particle diffusion rate through the sample than cold press method during heat treatment. Thus, chance of β phase formation of hot press method is greater than that of cold press method. The higher β phase fraction in hot pressed samples result in greater Seebeck coefficient than that of cold pressed samples.

Finally, we summarize our work and other publications to compare Seebeck coefficient result in Table 4-3.

Table 4-3: Summary Seebeck coefficient result of this work and other publications.

Publication	Composition	Preparation Method	Seebeck
This work	$Fe_{29.9}Cu_{0.1}Si_{70}$	MA for 50 hours, then hot pressed at 1173K with pressure of 26 MPa for 1 hour.	66 µV/K
This work	$Fe_{29.5}Cu_{0.5}Si_{70}$	MA for 50 hours, then pressed with pressure of 345 MPa. Finally, anneal at 1173K for 1 hour.	16 µV/K
Tsutsumi et al [10]	$Fe_{0.98}Co_{0.02}Si_2$	Plasma spray method, then annealing at 1123K for 40 hours.	-220 µV/K
Min et al [30]	$Fe_{0.95}Co_{0.05}Si_2$	MA for 50 hours, then hot pressed at 1153K with pressure of 50 MPa.	-183 µV/K
Umemoto [32]	$Fe_{28}Mn_2Si_{67}Al_3$	MA for 200 hours, then hot pressed at 1353K for 0.5 hour.	270 µV/K
Ito et al [50]	$Fe_{0.98}Co_{0.02}Si_2$	MA for 20 hours, then hot pressed at 1173 for 10 hours with pressure of 25 MPa.	-270 µV/K
Yamauchi et al [56]	$Fe_{27.86}Mn_1Si_{71.04}Cu_{0.1}$	Melt and solidification, then annealing at 1073K for 2.5 hours.	400 µV/K
Yamauchi et al [58]	$FeSi_2$	Melt and rapidly solidification, then annealing at 1163K for 20 hours.	80 µV/K
Tani et al [60]	$Fe_{0.9}Pt_{0.1}Si_2$	Melt and solidification, then annealing at 1113K for 168 hours.	-500 µV/K

CHAPTER V

CONCLUSION AND SUGGESTION

FeSi$_2$ were prepared by mechanical alloy (MA) technique using a planetary ball mill. Fe$_{30-x}$Cu$_x$Si$_{70}$ where x = 0, 1, 2 and 5 were selected instead of conventional composition, Fe$_{33.33}$Si$_{66.67}$, in order to avoid the metallic ε-FeSi phase. Each composition was milled for 50 hours, and then, was solidified by 2 methods. For the first method, the mixtures were cold compacted with 345 MPa gauge pressure, then annealed under Ar atmosphere at 1073K or 1173K. The annealing times were 1, 3 or 5 hours. For the second method, the mixtures were hot pressed with 26 MPa gauge pressure at 1173K and 1 hour soaking time. XRD was used to determine β and ε phase of the samples.

The β phase fraction and Seebeck coefficient of cold pressed samples increased with increasing of Cu content. Seebeck coefficient of cold pressed samples showed that 0.5%Cu sample when annealing at 1173K for 1 hour gives the highest Seebeck coefficient of 16µV/K at room temperature. Low Seebeck coefficient of cold pressed samples is due to the amount of metallic ε phase in cold pressed samples. This could be from unstablility of β phase and the remained large size of Fe powder in the mixture. At Fe rich zone, metallic ε phase could be developed.

Seebeck coefficient of all Cu-added hot pressed samples was greater than that of Cu free sample. For hot pressed samples, β phase fraction and Seebeck coefficient is maximize with content of Cu around 0.1% - 0.2%. In addition, Seebeck coefficient of hot pressed samples was greater than that of cold pressed samples. This could be from that the hot press method increase diffusion rate of particle during annealing. Chance of β phase formation of hot press method is greater than that of cold press method. In addition, Fe$_{(1-x)}$Cu$_x$Si$_2$ shown Seebeck coefficient greater than that of the conventional material of FeSi$_2$. Seebeck coefficient of hot pressed samples showed that 0.1%Cu sample gives the highest Seebeck coefficient of 66µV/K at room temperature.

The optimum %Cu added should be studied in future work. The %Cu with result of maximum Seebeck coefficient should be found out. The milling process should also be improved in order to get the small size around 1 μm of whole mixture as well as reduce milling time to save preparation cost. Lubricant in milling process should be more studied. The other kind of lubricant should be considered in future work. There might be possible to get small particle size of whole mixture and to continuous milling with non-stop to decrease preparation time and cost. However, contamination problem from the lubricant must be considered.

References

1. B. G. Min, and D. M. Rowe. Proceedings of 21st International Conference on Thermoelectronics. (2002): 365.

2. H. J. Goldsmid. Electronic Refrigeration. London: Pion, 1986.

3. D. M. Rowe, and C. M. Bhandari. Modern Thermoelectrics. London: Holt, Rinehalt and Winston Ltd., 1983.

4. D. M. Rowe ed. CRC Handbook of Thermoelectrics. Florida: CRC Press LLC, 1995.

5. C. M. Bhandari, and D. M. Rowe. Journal of Physics C. 11, (1978): 1787.

6. N. Savvides, and H. J. Goldsmid. Journal of Physics C. 13, (1980): 4671.

7. D. M. Rowe, and V. S. Shukla. Journal of Applied Physics. 52, (1981): 7421.

8. D. M. Rowe. Journal of Physics D. 7, (1974): 1843.

9. Y. Makita. AIP Conference Proceeding. 3 (1997): 404.

10. A. Tsutsumi, et al. Proceedings 17th International Conference on Themoelectrics. (1998): 410.

11. I. Nishida. Physics Review B. 7, (1973): 2710.

12. C. H. Holk, S. M. Yalisove, and G. L. Doll. Physics Review B. 52, (1995): 1692.

13. L. Miglio, and G. Malegori. Physics Review B. 52, (1995): 1448.

14. E. Arushanov, E. Bucher, Ch. Kloc, O. Kulikova, L. Kulyuk, and A. Siminel. Physics Review B. 52, (1995): 20.

15. U. Birkholtz, and J. Schelm. Fiz. Stat. Sol. 27, (1968): 413.

16. C. Kloc, E. Arushanov, M. Wendl, H. Hohl, U. Malang, and E. Bucher. Journal of Alloys and Compounds. 219, (1995): 93.

17. S. P. Murarka. Journal of Vacuum Science and Technology. 17, (1980): 775.

18. K. Uemura, and I. Nishida. Thermoelectric Semiconductors and Their Applications. Tokyo: Nikkan-Kogyo, 1998.

19. H. Nagai. Materials Transactions, JIM. 36, (1995): 365.

20. V. Borisenko ed. Semiconducting Silicides. Berlin: Springer, 2000.

21. R. M. Ware, and D. J. McNeill. Proceeding IEE. 111 (1964): 178.

22. T. Sakata, et al. Journal of Less-Common Metals. 61, (1978): 301.

23. I. Yamauchi, T. Okamoto, H. Ohata, and I. Ohnaka. Journal of Alloys and Compounds. 260, (1997): 162.

24. X. B. Zhao, T. J. Zhu, S. H. Hu, B. C. Zhou, and Z. T. Wu. Journal of Alloys and Compounds. 306, (2000): 303.

25. S. W. Kim, M. K. Cho, Y. Mishima, and D. C. Choi. Intermetallics. 11, (2003): 399.

26. W. S. Cho, T. Miyazaki, Y. Yoshihiko, and K. Hayashi. Journal of the Japan Institute of Metals. 60, (1996): 311.

27. W. S. Cho, S. W. Choi, and K. Park. Materials Science and Engineering. B 68 (1999): 116.

28. W. S. Cho , K. Park , S. W. Choi , and Y. S. Yoon. Materials Science and Engineering. B 76, (2000): 200.

29. E. Y. Belyaev, G. A. Suchkova, A. I. Ancharov, O. I. Lomovsky, and V. I. Maly. Proceedings 20th International Conference on Themoelectrics. (2001): 218.

30. B. G. Min, J. D. Shim, and D. H. Lee. Proceedings 17th International Conference on Themoelectrics. (1998): 386.

31. S. C. Ur, I. H. Kim, J. I. Lee, K. W. Cho, and P. Nash. Proceedings 21st International. Conference on Themoelectronics. (2002): 114.

32. M. Umemoto. Materials Transactions, JIM. 36, (1995): 373.

33. J. S. Benjamin. Metal Transaction. 1, (1970): 2943.

34. R. Sundaresan, and F. H. Froes. Journal of Metals. 39, (1987): 22.

35. H. R. Meddins, and J. E. Parrott. Journal of Physics C. 9, (1976): 1263.

36. H. Nagai, et al. Materials Transactions, JIM. 39, (1998): 515.

37. A. Sugiyama, et al. Journal of the Japan Institute of Metals. 62, (1998): 1082.

38. H. Shibata, et al. Proceedings 15th International Conference on Thermoelectrics. (1996): 62.

39. I. Yamauchi, T. Nagase, and I. Ohnaka. Journal of Alloys and Compounds. 292, (1999): 181.

40. I. Yamauchi, T. Nagase, and I. Ohnaka. Journal of Materials Science. 37, (2002): 1429.

41. A. F. Ioffe. Semiconductor Thermoelements and Thermoelectric Cooling. London: Inforseach Ltd., 1956.

42. K. Uemura, and I. A. Nishida. Thermoelectric Semiconductors and Its Applications. Tokyo: Nikkan-Kogyo Shinbun Ltd., 1988.

43. J. E. Parrot, and A. D. Stuckers. Thermal Conductivity of Solid. London: Pion, 1975.

44. I. A. Nishida. Proceedings of Japan-Russia-Ukraine International Workshop on Energy Conversion Materials, (ENECOM95), pp. 1. Japan, 1995.

45. O. Kubashewski. Iron-Binary Phase Diagrams. Berlin: Springer, 1982.

46. T. B. Massalsky ed. Binary alloy Phase Diagrams, ASM International. (1986): 1108.

47. T. Sakata, and I. Nishida. Bulletin of Japan Institute of Metals. 15, (1976): 1.

48. Y. Dusansoy, J. Protas, R. Wandij, and B. Roques. Acta Crystallographica B. 27, (1971): 1209.

49. T. Higashi, T. Nagase, and I. Yamauchi. Journal of Alloys and Compounds. 339, (2002): 96.

50. M. Ito, H. Nagai, E. Oda, S. Katsuyama, and K. Majima. Journal of Applied Physics. 91, (2002): 2138.

51. I. Yamauchi, T. Okamoto, and I. Ohnaka. Journal of Materials Science. 33, (1998): 371.

52. N. B. Elsner, C. H. Reynolds, C. C. Morris, and C. H. Shearer. Powder Metallurgy in Defense Technology. New Jersey: Rockaway, 1981.

53. B. A. Cook, B. J. Beaudry, J. L. Harringa, and W. J. Barnett. Proceedings of the 24th Intersociety of Energy Conversion Engineering Conference (IECEC), IEEE, pp. 693. Washington D.C., 1989.

54. R. M. German. Liquid Phase Sintering. New York: Plenum Publishing, 1985.

55. Jamreonta Parinyataramas. Synthesis of Cobalt doped β-FeSi2 by Mechanical Alloying. Master's Thesis, Department of Physics, Faculty of Science, Chulalongkorn University, 2006.

56. I. Yamauchi, A. Suganuma, T. Okamoto, and I. Ohnaka. Journal of Materials Science and Engineering. 32, (1997): 4603.

57. M. Tajima, and K. Hayashi. Journal of the Japan Society of Powder and Powder Metallurgy. 46, (1999): 757.

58. I. Yamauchi, S. Ueyama, and I. Ohnaka. Materials Science and Engineering A. 208, (1996): 108.

59. N. Sumida, T. Mishima, and H. Fujita. <u>Journal of Japan Institute of Metals.</u> 54, (1990): 1302.

60. J. Tani, and H. Kido. <u>Journal of Applied Physics.</u> 88, (2000): 5810.

VITAE

Name: Mr. Panuwat Attachotsakda

Date & Place of Birth: 9 July 1981, Bangkok, Thailand

Education: The 2nd Class Honours of Bachelor degree in Physics, Faculty of Science, Chulalongkorn University in 2002 academic year.

Working Experience:

Mar 2002 – Apr 2002:   Trainee as assistant researcher in Department of Physics at Office of Atomic Energy for Peace, Bangkok, Thailand. Research in "Study and Development of Neutron Shielding for Neutron diffractrometer" project.